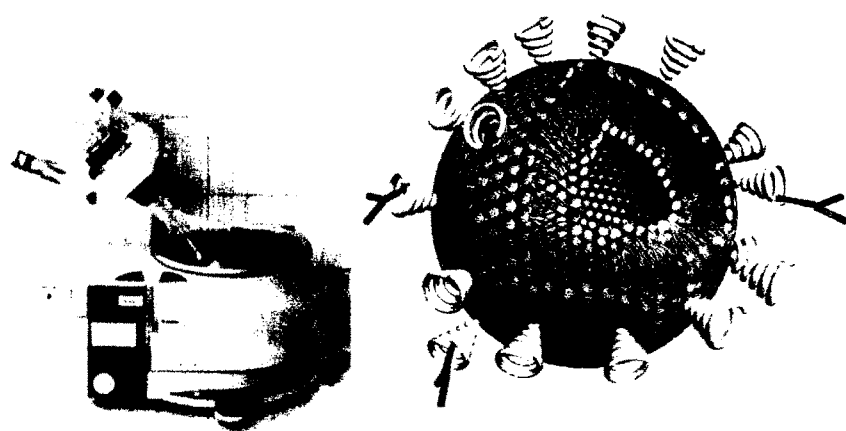


CHAPTER 4

FORMULATION OPTIMIZATION AND M6P-HSA CONJUGATION OF LIPOSOMES



Formulation Optimization and M6P-HSA Conjugation of Liposomes

4.1 INTRODUCTION

4.2 MATERIALS AND EQUIPMENTS

4.3 PREPARATION OF LIPOSOMES

4.3.1 Preparation of RGZ Liposomes by TFH Method

4.3.2 Formulation Optimization RGZ Loaded Liposomes Using Response Surface Methodology (RSM)

4.3.3 Preparation of CDS Liposomes by TFH Method

4.3.4 Formulation Optimization CDS Loaded Liposomes Using Response Surface Methodology (RSM)

4.4 PREPARATION OF M6P-HSA

4.5 CONJUGATION OF M6P-HSA TO LIPOSOMES

4.6 PARTICLE SIZE AND ZETA POTENTIAL OF UNCONJUGATED AND M6P- HSA CONJUGATED LIPOSOMES

4.7 TRANSMISSION ELECTRON MICROSCOPY (TEM)

4.8 LYOPHILIZATION OF LIPOSOMES AND OPTIMIZATION OF CRYOPROTECTANT CONCENTRATION

4.9 SOLID-STATE ANALYSIS

4.9.1 Differential Scanning Calorimetry (DSC):

4.9.2 X-ray Diffraction (XRD):

4.10 RESULTS AND DISCUSSION

4.10.1 Optimization of TFH Method Process Variables

4.10.2 Formulation Optimization RGZ Loaded Liposomes Using Response Surface Methodology (RSM)

4.10.2.1 Checkpoint Analysis

4.10.3 Formulation Optimization CDS Loaded Liposomes Using Response Surface Methodology (RSM)

4.10.3.1 Checkpoint Analysis

4.10.4 Preparation of M6P-HSA

4.10.5 Conjugation of M6P-HSA to Liposomes

4.10.6 Particle Size and Zeta Potential

4.10.7 Transmission Electron Microscopy (TEM)

4.10.8 Lyophilization of Liposomes and Optimization of Cryoprotectant

Concentration

4.10.9 Solid-state Analysis:

4.11 CONCLUSION

4.12 REFERENCES

4.1 INTRODUCTION

The liposomes are classified in to small unilamellar vesicles, large unilamellar vesicles, oligolamellar vesicles, and multi-lamellar vesicles. Various methods have been utilized for preparation of liposomes. There are at least fourteen major reported methods (Ostro, 1987; Martin et al., 1990(a)). The most commonly employed method are lipid film hydration also referred as thin film hydration method (TFH) (Bangham et al., 1965), reverse phase evaporation technique (REV) (Szoka and Papahadjopoulos, 1978; Sakai et al., 2008; Smirnov, 1984), rehydration-dehydration technique (Shew and Deamer, 1985; Seltzer et al., 1988; Kirby and Gregoriadis, 1984), ethanol injection method (Batzri and Korn, 1975; Jaafar-Maalej et al., 2010; Du and Deng, 2006; Maitani, 2010), ether infusion method (Deamer and Bangham, 1976; Cortesi et al., 1999), French press technique (Barenholz et al., 1979; Hamilton et al., 1980) and detergent dialysis technique (Matz and Jonas, 1982; Zumbuehl and Weder, 1981; Jiskoot et al., 1986; Ollivon et al., 2000). The difference lies between various methods of manufacture in the manner the membrane components are dispersed in aqueous media before being allowed to coalesce in the bilayer sheets form. In pharmaceutical point of view, the three most important aspects to be evaluated before selecting the method of preparation are the trapping efficiency, drug retention property and drug/lipid ratio (Betageri et al., 1993).

TFH method was selected for the preparation of liposomes in this investigation due to non-tediousness and feasible at lab scale compared to other techniques. Also, from the viewpoint of stability, the saturated phospholipid 1,2-Dilinoleoyl-sn-glycero-3-phosphocholine (DLPC), 1,2-diacyl-sn-glycero-3-phosphocholine (soy-hydrogenated) (HSPC), and 1,2-distearoyl-sn-glycero-3-phosphoethanolamine (DSPE) were used in this investigation. Trapping efficiency is one of the prime important factors in selection of method of liposome preparation. The trapping efficiency of 90% or more would be achieved with an optimum loading procedure. This necessitates the need for removal of untrapped drug because loading doses of 10% or less of free drug can usually be tolerated. Separation of untrapped or unincorporated drug (Betageri et al., 1993) from liposomes can be achieved either by 'gel filtration' (Sephadex mini-column centrifugation), ultra centrifugation, protamine aggregation, dialysis or controlled centrifugation at low speed. The free drug procedures, such as dialysis and

passage through exclusion columns, for removal of untrapped drug are often time-consuming, tedious, expensive, and makes recovery of untrapped drug difficult. Gel filtration was found to be very tenuous method with limited capacity and was not feasible for the entire formulation purification. Slight modification in the procedure was required for each specific liposome. Dialysis method was time consuming and was observed that drug leaks during the dialysis period. Protamine aggregation was destructive approach and its use is restricted for the determination of the drug entrapment and could not be used for the separation of the liposomal dispersion. Hence, controlled centrifugation at low speed was used in this investigation due to easy and faster method suitable for separation of untrapped drug.

Many lipid compositions can be employed for liposomal delivery systems; however, stability and cost are important determinants. Thus, acidic (negatively charged) lipids such as phosphatidyl serine, cardiolipin and phosphatidic acid are not preferred components as compared to phosphatidylcholine due to high costs and the often labile nature. Similarly, the use of unsaturated lipids, such as soya phosphatidylcholine or naturally occurring lipids, phosphatidylethanolamine and cardiolipin should be avoided due to its susceptibility towards oxidation. Thus, given similar loading and retention characteristics, liposomal systems composed of hydrogenated varieties of egg or soya phosphatidylcholine are pharmaceutically more preferred. Considering drug retention, it is unlikely that most drug-liposome formulations can exhibit sufficiently low leakage rates to allow retention times of one year or more (in dried or lyophilized form). However, if the trapping efficiencies are sufficiently high (e.g. 90% or more), removal of the untrapped drug may not be that necessary. No leakage of drug would then occur on extended storage due to absence of transmembrane drug concentration gradients. The optimum drug/lipid ratio of a liposomal formulation will likely be dictated by the biological efficacy and toxicity of the preparation and from a pharmaceutical point of view, high drug/lipid ratios are obviously more economical.

In summary, optimum liposomal formulations will exhibit drug trapping efficiencies of more than 90%, employ inexpensive and relatively saturated lipids and cholesterol and using highest possible drug/lipid ratio results in consistent and maintained efficacy of the preparation. Apart from these factors; other factors which need to be

considered in selection of the methods of preparation include selection of methods which would avoid the use of organic solvents and detergents which are difficult to remove, yield well-defined and reproducible liposomes and which are rapid and feasible for scale up procedures. Selection of the appropriate method is also dependent on applications of the liposomes. In the stabilization of liposomes using freeze or spray drying technique there is a basic necessity, that is sufficient rigidity in the liposomal membrane to withstand drying with minimum or least leakage of the entrapped drug.

Mannose 6-phosphate/ insulin like growth factor II (M6P/IGF II) receptor are over expressed on the surface of HSCs during liver fibrosis. Mannose 6-phosphate modified human serum albumin (M6P-HSA) is selective to M6P/IGF II receptor and thus accumulates in activated HSCs of fibrotic liver. M6P-HSA as such has been investigated as a carrier for a number of drugs, including pentoxifylline (Gonzalo et al., 2006), mycophenolic acid (Greupink et al., 2005), doxorubicine (Greupink et al., 2006) and gliotoxin (Hagens et al., 2006). M6P-HSA conjugated liposomes can be used as HSCs selective carrier of antifibrotic drugs to improve the efficacy of drugs at the same time to reduce their adverse effects. Liposomes with few parts of bioactive lipid dilinoleoylphosphatidylcholine (DLPC) into the membrane act as a bioactive drug carrier which can deliver drugs and simultaneously have beneficial antifibrotic effects (Beljaars et al., 1999; Beljaars et al., 2001; De Bleser et al., 1996; De Bleser et al., 1995; Adrian et al., 2006; Cao et al., 2002).

This chapter demonstrates the preparation of liposomes considering the above discussed factors. Liposomes of Rosiglitazone (RGZ), and Candesartan (CDS) were prepared using TFH technique with membrane composition consisting of lipids such as DLPC, HSPC, DSPE and cholesterol. Various formulation variables are optimized to achieve desired response variables using factorial design and response surface methodology (RSM). Prepared liposomes were characterized for size and size distribution, zeta potential, percent drug Entrapment (PDE) and percentage reduction (PR) in PDE after 10 days kept at refrigerated condition.

4.2 MATERIALS AND EQUIPMENTS

1,2-Dilinoleoyl-sn-glycero-3-phosphocholine (DLPC), 1,2-diacyl-sn-glycero-3-phosphocholine (soy-hydrogenated) (HSPC), and 1,2-distearoyl-sn-glycero-3-phosphoethanolamine (DSPE) were obtained as a gift sample from Genzyme Pharmaceuticals, Switzerland. RGZ as a PPAR γ ligand was obtained as a gift sample from Zydu Research Center, Ahmedabad, India. CDS was obtained as a gift sample from Alembic Research Center, Vadodara, India. Cholesterol (CH) ($\geq 99\%$) was purchased from Sigma-Aldrich Corporation, Bangalore, India. Cholesterol (CH) ($\geq 99\%$), human serum albumin ($\geq 96\%$, lyophilized powder, Mw 66478 Da), 4-Nitrophenyl α -Dmannopyranoside, sebacic acid, and dialysis tubing cellulose membrane (Mw cutoff 12400 Da) were purchased from Sigma-Aldrich Corporation, Bangalore, India. N,N-dicyclohexyl carbodiimide (DCCI) and 1-(3-dimethylamino propyl)-3-ethylcarbodiimide hydrochloride (EDCI) were purchased from Himedia Laboratories, Mumbai, India. Chloroform (LiChrosolv®) and methanol (LiChrosolv®) were purchased from Merck specialties limited, Mumbai, India. Mannitol, Sucrose, Lactose, Trehalose and Glycine were purchased from Himedia Laboratories, Mumbai, India. polycarbonate membrane filter (1 μ m, 0.4 μ m, 0.2 μ m and 0.1 μ m) were purchased from Whatman, Mumbai, India. All other reagents used were of analytical grade. Water used was distilled and prefiltered through 0.2 μ m filter.

The equipments such as rotary evaporator with vacuum pump and thermostatically controlled water bath and nitrogen purging facility (Superfit Equipments, India); Analytical balance (Precisa 205A SCS, Switzerland); high-pressure extruder (Avestin® EmulsiFlex- C5 with extruder, Avestin Inc., Ottawa, Canada); pH meter (Systronics 335, India); Cyclomixer, three blade stirrer (Remi Scientific Equipments, Mumbai); Cooling Centrifuge (Sigma Laboratory centrifuge, 3 K 30, Osterode, GmbH); Water bath, Magnetic stirrer and heating mantle (Remi, Mumbai); UV-Visible Spectrophotometer, (Shimadzu UV-1700, Japan); Vacuum Pump F16, (Bharat Vacuum pumps, Bangalore); Optical microscope with polarizer (BX 40, Olympus Optical Co. Ltd., Japan); Malvern Zetasizer analyzer (NanoZS, Malvern Instruments, UK), Karl fisher Auto-titrater [Toshiwal Instruments (Bombay) Pvt. Ltd., Nasik] FTIR spectrophotometer (BRUKER, α -Alpha T, Germany) were used.

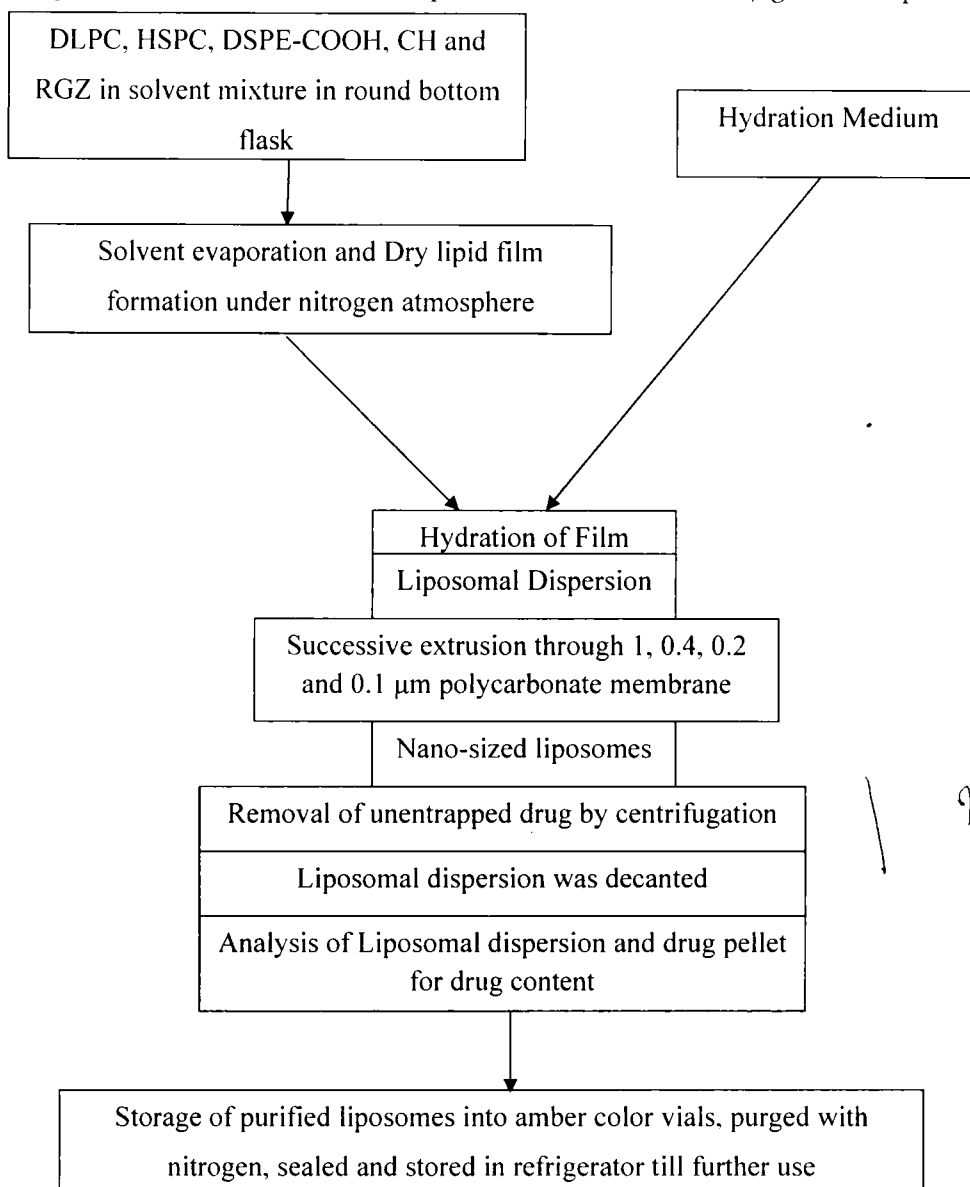
4.3 PREPARATION OF LIPOSOMES

4.3.1 Preparation of RGZ Liposomes by TFH Method

Liposomes of RGZ consisting of DLPC, HSPC, DSPE-COOH and CH were prepared by TFH technique (New, 1990). Briefly, the lipids and RGZ were dissolved in a mixture of chloroform and methanol (ratio 4:1 v/v) in a 250ml round bottom flask in different molar ratios. The solvent was evaporated in the rotary flash evaporator. The thin dry lipid film thus formed was hydrated using purified water at 65°C. The size of liposomes was reduced using successive extrusion through 1, 0.4, 0.2 and 0.1 µm polycarbonate membrane filter using Avestin high-pressure extruder. Untrapped free drug in the liposomal dispersion was separated by centrifuging (Sigma Laboratory centrifuge, 3 K 30, Osterode, GmbH) liposomal suspension at 7500 rpm (4779 g) for 2 minutes. Liposomal suspension was decanted and drug pellet was separated. Liposomal suspension was then characterized for vesicle size, size distribution (in term of poly dispersity index) and zeta potential using Malvern Zetasizer vesicle size. The encapsulation efficiency of RGZ liposomes was determined by dissolving known quantity of liposomes (after separation of free drug) in methanol and estimating drug content by UV/VIS spectrophotometric method (As discussed in chapter 3). Mass balance was evaluated by measuring untrapped drug in pellet. A flowchart depicting the process is shown in scheme 4.1. The liposomal compositions and process parameters were optimized to achieve maximum drug entrapment.

PDE was calculated using the formula:

$$\text{PDE} = \frac{\text{Amount of Drug Encapsulated in Liposomes}}{\text{Amount of Drug Used in Liposome Preparation}} \times 100$$



Scheme 4.1 TFH process stages in the preparation of RGZ liposomes

4.3.2 Formulation Optimization RGZ Loaded Liposomes Using Response Surface Methodology (RSM)

The RGZ loaded liposomal formulations were optimized using 3^3 full factorial design by varying drug: lipid molar ratio (1:15, 1:20 and 1:25), lipid: cholesterol molar ratio (9:1, 8:2 and 7:3), and total solid content: volume of hydration media ratio (1:10, 1:12.5 and 1:15) at 3 different levels as low (-1), medium (0) and high (1), by keeping all other process and formulation parameter invariant, to maximize PDE and to

minimize PR in PDE after 10 days kept at refrigerated condition (Cochran and Cox, 1992). The response variables considered for formulation optimization were PDE and PR in PDE (Fannin et al., 1981; Subramanian et al., 2004; Padamwar and Pokharkar, 2006; Loukas, 1997; Vali et al., 2008; Murthy and Umrethia, 2004; Seth and Misra, 2002; Gonzalez-Mira et al., 2011; Gonzalez-Rodriguez et al., 2007).

Table 4.1 Coded Values of the formulation parameters

Coded value	Actual value		
	X1	X2	X3
-1	1:15	9:1	1:10
0	1:20	8:2	1:12.5
1	1:25	7:3	1:15

X1 = Drug: Lipid molar ratio

X2 = Lipid: Cholesterol molar ratio

X3 = Total solid content: Volume of hydration media ratio

RSM was applied using comprehensive software, Design-Expert®8.0.4 (Stat-Ease Inc., MN) to fit second order polynomial equations, obtained by multiple linear regression analysis (MLRA) approach. A full and reduced model for both PDE and PR was established by putting the values of regression coefficients in polynomial equation. Statistical soundness of the polynomial equations was established on the basis of analysis of variance (ANOVA) statistics (Anthony Armstrong and James, 1996; Singh et al., 2005(c); Stensrud et al., 2000; Xiong et al., 2009; Singh et al., 2005(b); Singh et al., 2005(a); Naik et al., 2010; Ducat et al., 2010).

Two dimensional contour plots and three dimensional response surface plots (Box and Wilson, 1951; Box et al., 1978; Kenneth et al., 1995) were established by varying levels of two factors and keeping the third factor at fixed levels at a time. In this way, they are more helpful in understanding the actual interaction amongst the varying factors on the response parameter and are more meaningful. The 2-D contour plots and 3-D response surface graphs were constructed using the Design Expert software.

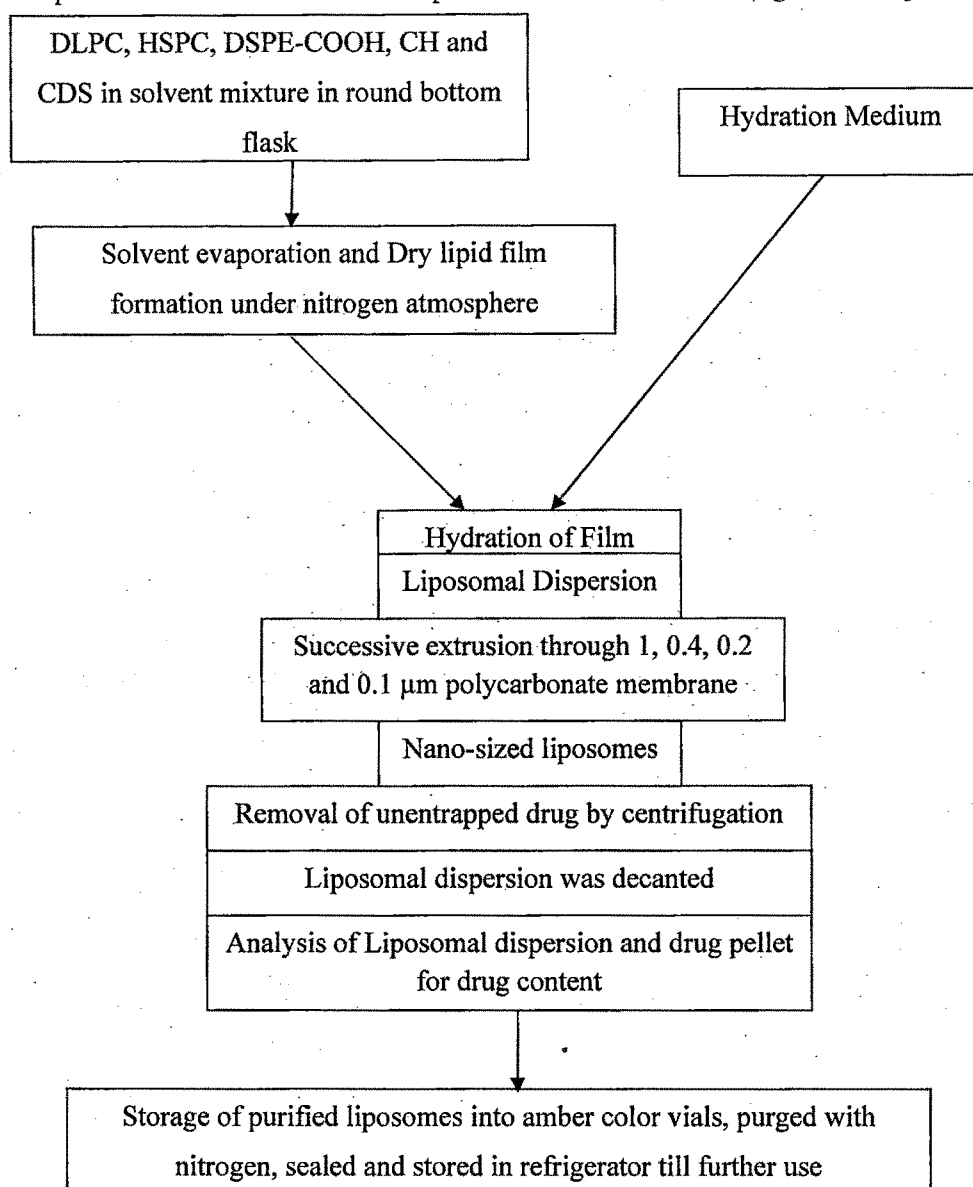
The experimental design and the derived polynomial equation for the optimization of liposomal formulation were validated for their utility by performing check point analysis. Eight optimum checkpoints were selected, prepared and evaluated for response parameters i.e. PDE and PR. Statistical comparison between the predicted

values and average of three experimental values of the response parameters was performed to derive percentage error and to evaluate significant difference between these values.

Optimized formulation was derived by specifying goal and importance to the formulation variables and response parameters. Results obtained from the software were further verified by actual preparation of the batches and comparing the predicted and actual results.

4.3.3 Preparation of CDS Liposomes by TFH Method

Liposomes of CDS consisting of DLPC, HSPC, DSPE-COOH and CH were prepared by TFH technique (New, 1990). Briefly, the lipids and CDS were dissolved in a mixture of chloroform and methanol (ratio 4:1 v/v) in a 250ml round bottom flask in different molar ratios. The solvent was evaporated in the rotary flash evaporator. The thin dry lipid film thus formed was hydrated using purified water at 65°C. The size of liposomes was reduced using successive extrusion through 1, 0.4, 0.2 and 0.1 μm polycarbonate membrane filter using Avestin high-pressure extruder. Untrapped free drug in the liposomal dispersion was separated by centrifuging (Sigma Laboratory centrifuge, 3 K 30, Osterode, GmBH) liposomal suspension at 7500 rpm (4779 g) for 2 minutes. Liposomal suspension was decanted and drug pellet was separated. Liposomal suspension was then characterized for vesicle size, size distribution (in term of poly dispersity index) and zeta potential using Malvern Zetasizer vesicle size. The encapsulation efficiency of RGZ liposomes was determined by dissolving known quantity of liposomes (after separation of free drug) in methanol and estimating drug content by UV/VIS spectrophotometric method (As discussed in chapter 3). Mass balance was evaluated by measuring untrapped drug in pellet. A flowchart depicting the process is shown in scheme 4.2. The liposomal compositions and process parameters were optimized to achieve maximum drug entrapment.



Scheme 4.2 TFH process stages in the preparation of CDS liposomes

4.3.4 Formulation Optimization CDS Loaded Liposomes Using Response Surface Methodology (RSM)

The liposomal formulations were optimized using 3^3 full factorial design by varying Drug: Lipid molar ratio (1:15, 1:20 and 1:25), Lipid: Cholesterol molar ratio (9:1, 8:2 and 7:3), and total solid content: volume of hydration media (1:10, 1:12.5 and 1:15) at 3 different levels as low (-1), medium (0) and high (1), by keeping all other process and formulation parameter invariant, to maximize PDE and to minimize percentage

reduction (PR) in PDE after 10 days kept at refrigerated condition (Cochran and Cox, 1992). The response variables considered for formulation optimization were PDE and PR in PDE. (Fannin et al., 1981; Subramanian et al., 2004; Padamwar and Pokharkar, 2006; Loukas, 1997; Vali et al., 2008; Murthy and Umrethia, 2004; Seth and Misra, 2002; Gonzalez-Mira et al., 2011; Gonzalez-Rodriguez et al., 2007)

Table 4.2 Coded Values of the formulation parameters

Coded value	Actual value		
	X1	X2	X3
-1	1:15	9:1	1:10
0	1:20	8:2	1:12.5
1	1:25	7:3	1:15

X1 = Drug: Lipid molar ratio

X2 = Lipid: Cholesterol molar ratio

X3 = Total solid content: Volume of hydration media

RSM was applied using comprehensive software, Design-Expert 8.0.4 (Stat-Ease Inc., MN) to fit second order polynomial equations, obtained by multiple linear regression analysis (MLRA) approach. A full and reduced model for both PDE and PR was established by putting the values of regression coefficients in polynomial equation. Statistical soundness of the polynomial equations was established on the basis of ANOVA statistics (Anthony Armstrong and James, 1996; Singh et al., 2005(c); Stensrud et al., 2000; Xiong et al., 2009; Singh et al., 2005(b); Singh et al., 2005(a); Naik et al., 2010; Ducat et al., 2010).

Two dimensional contour plots and three dimensional response surface plots (Box and Wilson, 1951; Box et al., 1978; Kenneth et al., 1995) were established by varying levels of two factors and keeping the third factor at fixed levels at a time. In this way they are more helpful in understanding the actual interaction amongst the varying factors on the response parameter and are more meaningful. The 2-D contour plots and 3-D response surface graphs were constructed using the Design Expert software.

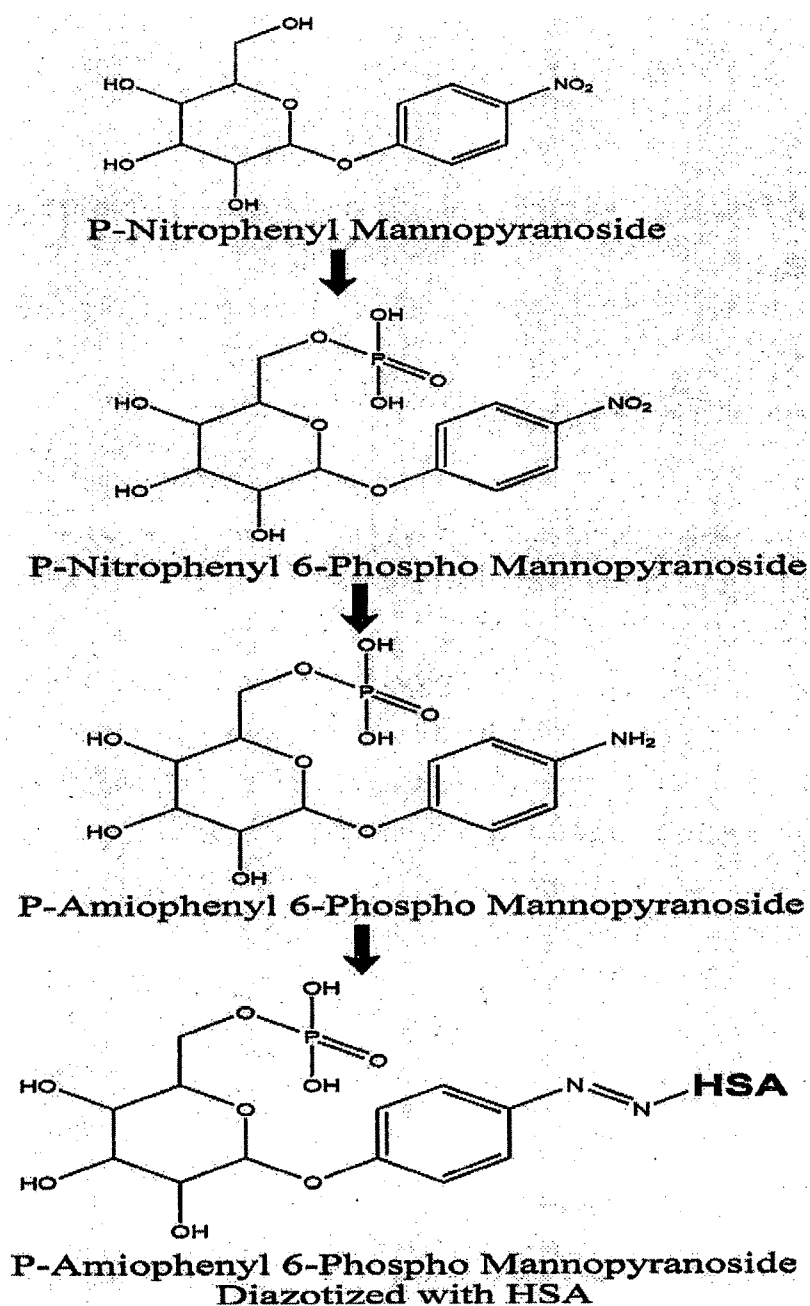
The experimental design and the derived polynomial equation for the optimization of liposomal formulation were validated for their utility by performing check point analysis. Eight optimum checkpoints were selected, prepared and evaluated for response parameters i.e. PDE and PR. Statistical comparison between the predicted

values and average of three experimental values of the response parameters was performed to derive percentage error and to evaluate significant difference between these values.

Optimized formulation was derived by specifying goal and importance to the formulation variables and response parameters. Results obtained from the software are further verified by actual preparation of the batches and comparing the predicted and actual results.

4.4 PREPARATION OF M6P-HSA

M6P-HSA was synthesized and characterized. Firstly, p-nitrophenyl- α -D-mannopyranoside was phosphorylated by reacting with phosphoryl chloride (Roche et al., 1985) to get p-nitrophenyl-6-phospho- α -D-mannopyranoside whose p-nitro group was further reduced with 10% palladium on active carbon under a hydrogen atmosphere of 1 atm (Monsigny et al., 1984) to obtain p-aminophenyl-6-phospho- α -D-mannopyranoside, which was then coupled to HSA by diazo bond formation (Kataoka and Tavassoli, 1984). Prepared M6P-HSA was purified, characterized for protein content (Colorimetric estimation at 550 nm after reacting with Biuret reagent in alkaline medium), number of M6P molecules (colorimetric estimation at 490 nm after reaction with phenol in presence of sulfuric acid) and number of phosphate groups coupled to each HSA molecules (Colorimetric estimation at 830 nm after reacting with ammonium molybdate – sulfuric acid reagent, 1-Amino 2-naphthyl 4-sulfonic acid reagent and hydrogen peroxide), lyophilized and stored at -20 °C till further use (Dubois et al., 1956; Bottcher et al., 1961)

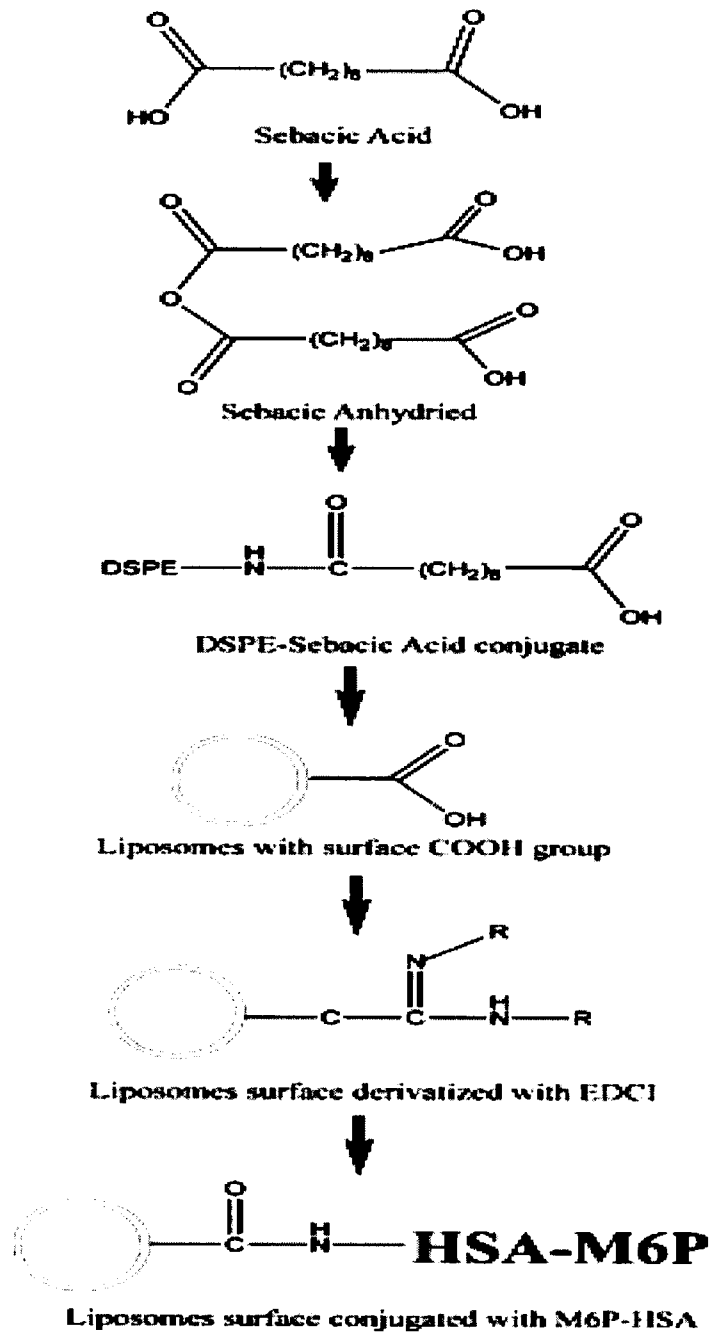


Scheme 4.3 Synthesis of M6P-HSA

4.5 CONJUGATION OF M6P-HSA TO LIPOSOMES

M6P-HSA was conjugated to liposomes containing DSPE-COOH by EDCI method as described by Martin et al., 1990(a). First of all, liposomal suspension was activated for an hour with EDCI (2.5mg/ml) in phosphate buffered saline pH 5. Add 50 μ l of M6P-HSA solution (10 mg/ml) to each milliliter of liposome suspension (DSPE-

COOH 0.05 $\mu\text{mol/ml}$). Ionic strength was increased by adding 50 μl of 1 M sodium chloride solution and adjusting the pH at pH 8. The reaction was carried out over night at 4 $^{\circ}\text{C}$. Particle size and zeta-potential of M6P-HSA liposomes were determined.



1029

Scheme 4.4 M6P-HSA Conjugation to Liposomes

4.6 PARTICLE SIZE AND ZETA POTENTIAL OF UNCONJUGATED AND M6P-HSA CONJUGATED LIPOSOMES

The size of Liposomes was measured by dynamic light scattering with a Malvern Zetasizer. Diluted liposome suspension was added to the sample cuvette and then cuvette is placed in zetasizer. Sample is stabilized for two minutes and reading was measured. The average particle size was measured after performing the experiment in triplicate. The zeta potential of developed liposomes was determined using Malvern Zetasizer. The zeta potential was calculated by Smoluchowski's equation from the electrophoretic mobility of liposomes at 25 °C (Mu and Feng, 2001).

4.7 TRANSMISSION ELECTRON MICROSCOPY (TEM)

The unconjugated and M6P-HSA conjugated liposomal vesicles were observed by TEM to illustrate their ultrastructure. A drop of liposome samples were applied to a carbon film-covered copper grid to form a thin film, which was then stained with 1% phosphotungstic acid. The samples were then observed with a Tecnai 20 transmission electron microscope (PHILIPS, Holland) (Zasadzinski, 1986).

4.8 LYOPHILIZATION OF LIPOSOMES AND OPTIMIZATION OF CRYOPROTECTANT CONCENTRATION

The liposomal suspensions have thermodynamic instability upon storage and lead to drug leakage and formation of aggregates. Freeze drying/ lyophilization is one of the known methods to recover the liposomes in the dried form and suitably redisperse the cake at time of administration. The liposomal suspension was stabilized by lyophilization. The dispersion was frozen at -70 °C and dried under negative displacement pressure (Heto Drywinner model DW1 0-60E, Denmark), for 24 h. Different cryoprotectants at various ratios and anti-adherent are evaluated. The lyophilized formulations were tested for particle size, zeta potential and percentage drug retention (PDR) (Ozer and Talsma, 1989; Hinrichs et al., 2006; Nounou et al., 2005; Crowe et al., 1985; Hernandez Caselles et al., 1990; Patel et al., 2009).

4.9 SOLID-STATE ANALYSIS

Differential Scanning Calorimetry (DSC) studies and X-ray Diffraction (XRD) studies were conducted for lyophilized batches of M6P-HSA conjugated liposomes.

The main objective of these studies was to determine possible changes in crystallinity of drug after incorporation into liposomes.

4.9.1 Differential Scanning Calorimetry (DSC)

DSC experiments were carried out using differential thermal analyzer (Mettler Toledo star® SW 7.01, USA) to evaluate thermal properties and to characterize the physical state of drugs in pure form and in liposomal formulations. Five to ten milligrams of pure drug and its liposomes were put separately in aluminum pan and hermetically sealed. The heating rate was adjusted at 10°C/min, nitrogen was used as purging gas and liquid nitrogen was employed to cool down the system (Yousefi et al., 2009; Atyabi et al., 2009; Crosasso et al., 2000; Van Winden et al., 1998).

4.9.2 X-ray Diffraction (XRD)

XRD was carried out with a BRUKER (D8 Advance, Germany) diffractometer. The diffraction patterns were recorded over 2θ angular range of 3°-35° with a scan speed of 2°/min at room temperature (Cavalcanti et al., 2007; Patil and Gaikwad, 2009).

4.10 RESULTS AND DISCUSSION

Liposomal formulations of RGZ and CDS were prepared by the selected TFH method using DLPC, HSPC, DSPE-COOH and CH, were optimized to maximize PDE and minimize PR in PDE. Drugs entrapment in to liposomes involved co-evaporation of the lipid and drug from the solvent system in a round bottom flask. First of all, various process variables were optimized and then formulation variables were optimized using RSM. The results are summarized and discussed in the following sections.

4.10.1 Optimization of TFH Method Process Variables

Process variables, such as vacuum conditions for dry film formation, hydration time, and speed of rotation of flask were optimized for desired results. The effect of one variable was studied at a time keeping other variables constant. The results are recorded in Table 4.3 from which the following conclusions are drawn:

1. The vacuum required for solvent evaporation to form a uniform thin film was raised from 400 mm Hg to 650 mm Hg. The low vacuum (400 mm Hg) was found to be insufficient for the complete removal of the solvent mixture. The presence of residual solvent may lead to physical destabilization of liposomes

by interfering with the co-operative hydrophobic interactions among the phospholipid methylene groups that hold the structure together (Martin et al., 1990(a)). The vacuum of 600 mm of Hg for 60 minutes was found to be optimum for complete evaporation of solvent mixture and producing more translucent and thin lipid film. However, for complete solvent removal of residual solvent (post film formation) the flask was kept in a desiccator for 24 hrs containing activated silica. Higher vacuum (650 mm Hg) resulted in rapid evaporation of the solvent system leading to crystallization of the drug and hence resulted in poor percent drug entrapment in the liposomes. This is in agreement with the findings of Martin et al (1990) that differential solubilities of amphiphilic components of bilayer and drug in organic solvents are often encountered and must be taken into consideration in order to avoid crystallization of a single component during solvent-stripping operations.

2. Speed of rotation: The speed of rotation of flask was increased from 50 rpm to 150 rpm. Rotation of 50 rpm resulted in thick incompletely dried film and presence of residual solvents. While at 150-rpm speed, a dry film with varying thickness was produced with a thicker film at periphery and thinner film at the center. A speed of 100 rpm was found to be adequate to give thin, uniform and completely dry film. Hence, 100-rpm speed of rotation of flask was selected to be optimum for liposomal preparations.
3. Hydration time: The lipid film was hydrated from 30 minutes to 2 hours before size reduction. An optimal hydration time was required for complete conversion of planar bilayers to spherical liposomes. Lower hydration time led to a non-uniform shape and size of the liposomes and also the un-hydrated part posed difficulty in size reduction. The hydration time beyond 1 h resulted in no further improvement. Hence, 1 hr hydration time was found to be optimum for both RGZ and CDS liposome preparation.



Table 4.3 Selection of process parameters by TFH method for RGZ and CDS liposomes

	RGZ	CDS
COMPOSITION OF SOLVENT SYSTEM		
CHLOROFORM: METHANOL	Observation	
1:1	No proper film, not proper hydration	No proper film, not proper hydration
2:1	No proper film, not proper hydration	No proper film, not proper hydration
1:2	No proper film, not proper hydration	No proper film, not proper hydration
4:1	Suitable	Suitable
SOLVENT EVAPORATION TIME		
Time (minutes)	Observation	
45 minutes	Not proper hydration	Not proper hydration
60 minutes	Suitable (Solvent is completely removed)	Suitable (Solvent is completely removed)
90 minutes	No further improvement	No further improvement
SPEED OF ROTATION		
rpm	Observation	
50 rpm	Non Uniform distribution	Non Uniform distribution
100 rpm	Suitable	Suitable
150 rpm	Non Uniform distribution	Non Uniform distribution
HYDRATION TIME		
Time (min)	Observation	
30 minutes	Not properly hydrated	Not properly hydrated
60 minutes	Suitable hydration	Suitable hydration
90 minutes	No further improvement but decrease in PDE	No further improvement but decrease in PDE
VACUUM APPLIED		
vacuum (mm of Hg)	Observation	
400	Flecking during hydration	Flecking during hydration
500	Flecking during hydration	Flecking during hydration
600	Uniform film and uniform liposomal dispersion	Uniform film and uniform liposomal dispersion
650	Un-uniform film	Un-uniform film

4.10.2 Formulation Optimization RGZ Loaded Liposomes Using Response Surface Methodology (RSM)

All twenty seven batches of liposomes were prepared according to the formulation variables as shown in Table 4.4. All formulations were evaluated for PDE and PR and the results obtained are shown in Table 4.4.

Table 4.4 3³ Full factorial design outline with results for PDE and PR. The data represent the mean ± SEM (n = 3).

Batch No.	X1	X2	X3	X1 ²	X2 ²	X3 ²	X1X2	X2X3	X1X3	X1X2 X3	PDE (mean ^a ± SEM)	PR (mean ^a ± SEM)
1	0	0	-1	0	0	1	0	0	0	0	79.79 ± 1.272	2.99 ± 0.051
2	0	0	0	0	0	0	0	0	0	0	78.24 ± 0.944	2.63 ± 0.070
3	0	0	1	0	0	1	0	0	0	0	69.70 ± 0.962	2.84 ± 0.063
4	0	-1	-1	0	1	1	0	1	0	0	81.83 ± 0.916	4.55 ± 0.096
5	0	-1	0	0	1	0	0	0	0	0	80.63 ± 0.848	4.14 ± 0.091
6	0	-1	1	0	1	1	0	-1	0	0	75.84 ± 1.024	5.25 ± 0.116
7	0	1	-1	0	1	1	0	-1	0	0	75.13 ± 0.957	2.20 ± 0.067
8	0	1	0	0	1	0	0	0	0	0	73.23 ± 1.122	2.32 ± 0.074
9	0	1	1	0	1	1	0	1	0	0	61.23 ± 0.638	2.32 ± 0.069
10	-1	0	-1	1	0	1	0	0	1	0	60.34 ± 0.886	2.67 ± 0.084
11	-1	0	0	1	0	0	0	0	0	0	58.00 ± 0.769	3.84 ± 0.098
12	-1	0	1	1	0	1	0	0	-1	0	51.52 ± 0.950	3.16 ± 0.084
13	-1	-1	-1	1	1	1	1	1	1	-1	65.15 ± 0.770	6.05 ± 0.139
14	-1	-1	0	1	1	0	1	0	0	0	62.61 ± 0.734	5.59 ± 0.120
15	-1	-1	1	1	1	1	1	-1	-1	1	55.62 ± 0.824	5.16 ± 0.117
16	-1	1	-1	1	1	1	-1	-1	1	1	52.50 ± 0.722	2.32 ± 0.065
17	-1	1	0	1	1	0	-1	0	0	0	51.17 ± 0.758	2.72 ± 0.063
18	-1	1	1	1	1	1	-1	1	-1	-1	44.06 ± 0.696	2.77 ± 0.077
19	1	0	-1	1	0	1	0	0	-1	0	79.66 ± 0.935	2.81 ± 0.067
20	1	0	0	1	0	0	0	0	0	0	78.39 ± 0.988	2.62 ± 0.058
21	1	0	1	1	0	1	0	0	1	0	68.43 ± 0.837	3.01 ± 0.080
22	1	-1	-1	1	1	1	-1	1	-1	1	83.01 ± 1.119	5.29 ± 0.104
23	1	-1	0	1	1	0	-1	0	0	0	82.16 ± 1.050	6.16 ± 0.132
24	1	-1	1	1	1	1	-1	-1	1	-1	75.32 ± 1.141	5.46 ± 0.121
25	1	1	-1	1	1	1	1	-1	-1	-1	73.78 ± 0.984	2.09 ± 0.051
26	1	1	0	1	1	0	1	0	0	0	72.25 ± 0.852	2.12 ± 0.058
27	1	1	1	1	1	1	1	1	1	1	60.02 ± 0.746	2.22 ± 0.079

A full model for both PDE and PR was established by putting the values of intercepts and regression coefficients in polynomial equation.

PDE Full equation

$$Y_{\text{PDE}} = 78.14468 + 9.558367 X_1 - 5.48965 X_2 - 4.96913 X_3 - 9.84887 X_1^2 - 1.25302 X_2^2 - 3.35766 X_3^2 + 0.099888 X_1 X_2 - 1.07391 X_2 X_3 - 0.49006 X_1 X_3 - 0.8949 X_1 X_2 X_3$$

PR Full equation

$$Y_{\text{PR}} = 2.714256 - 0.13946 X_1 - 1.47617 X_2 + 0.068833 X_3 + 0.421645 X_1^2 + 0.866131 X_2^2 - 0.06424 X_3^2 - 0.12592 X_1 X_2 + 0.059925 X_2 X_3 + 0.037889 X_1 X_3 - 0.17164 X_1 X_2 X_3$$

The Model F-value of 284.38 and 24.47 respectively for PDE and PR implies the model is significant. For both PDE and PR, there is only a 0.01% chance that a

"Model F-Value" this large could occur due to noise. Values of "Probability value > F" less than 0.0500 indicate model terms are significant. In the case of PDE X_1 , X_2 , X_3 , X_2X_3 , X_1^2 , X_2^2 , X_3^2 and $X_1X_2X_3$ and in the case of PR X_2 , X_1^2 , X_2^2 are significant model terms. Values greater than 0.1000 indicate the model terms are not significant. If there are many insignificant model terms model reduction may improve the model.

PDE Reduced equation

$$Y_{PDE} = 78.14468 + 9.558367 X_1 - 5.48965 X_2 - 4.96913 X_3 - 9.84887 X_1^2 - 1.25302 X_2^2 - 3.35766 X_3^2 - 1.07391 X_2X_3 - 0.8949 X_1X_2X_3$$

PR Reduced equation

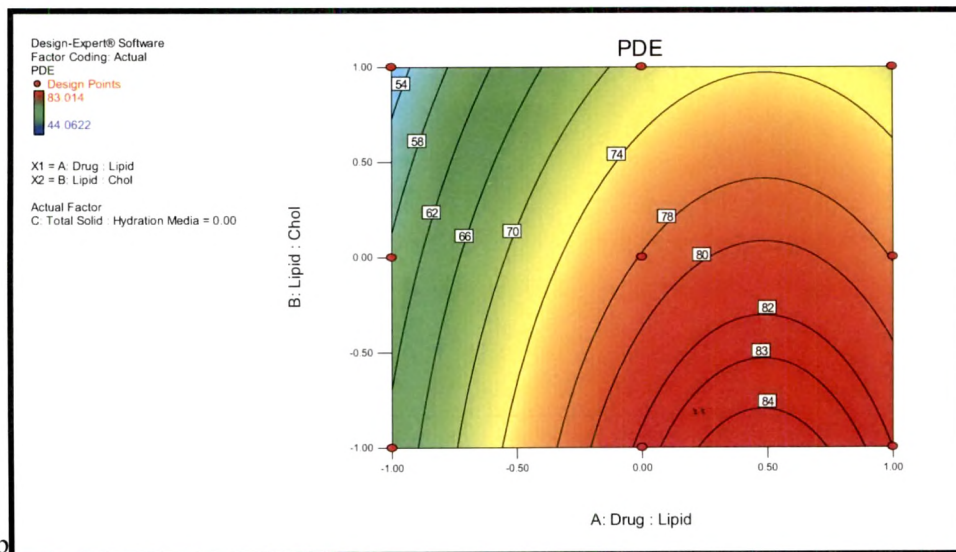
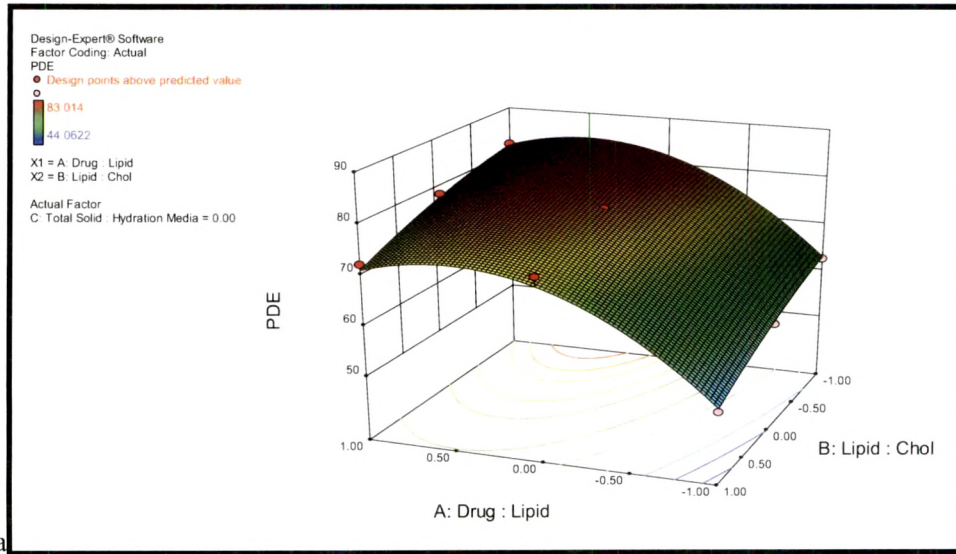
$$Y_{PR} = 2.671429 - 1.47617 X_2 + 0.421645 X_1^2 + 0.866131 X_2^2$$

The "Predicted R-Squared" of 0.9802 is in reasonable agreement with the "Adjusted R-Squared" of 0.9909 in case of PDE and the "Predicted R-Squared" of 0.8418 is in reasonable agreement with the "Adjusted R-Squared" of 0.9003 in the case of PE. "Adequate Precision" measures the signal to noise ratio. A ratio greater than 4 is desirable. The ratio of 56.661 for PDE and 13.470 for PR indicates an adequate signal. This model can be used to navigate the design space.

Comparison of full model (FM) and reduced model (RM) was done by ANOVA by applying the F-Statistic to check effect of omission of the statistically insignificant coefficients from the full model and the results are shown in Table 4.5.

Table 4.5 Analysis of Variance (ANOVA) of full and reduced models

Response	Model		df	SS	MS	F	Adjusted R ²	Predicted R ²	ANOVA comparison	
									F Calculated	F Tabulated
PDE	Regression	FM	10	3313.75	331.38	284.38	0.9909	0.9802	1.2880	3.63
		RM	8	3310.75	413.84	344.14				
	Residual (Error)	FM	16	18.64	1.17					
		RM	18	21.65	1.20					
PE	Regression	FM	10	45.74	4.57	24.47	0.9003	0.8418	0.7233	2.66
		RM	3	44.79	14.93	87.23				
	Residual (Error)	FM	16	2.99	0.19					
		RM	23	3.94	0.17					



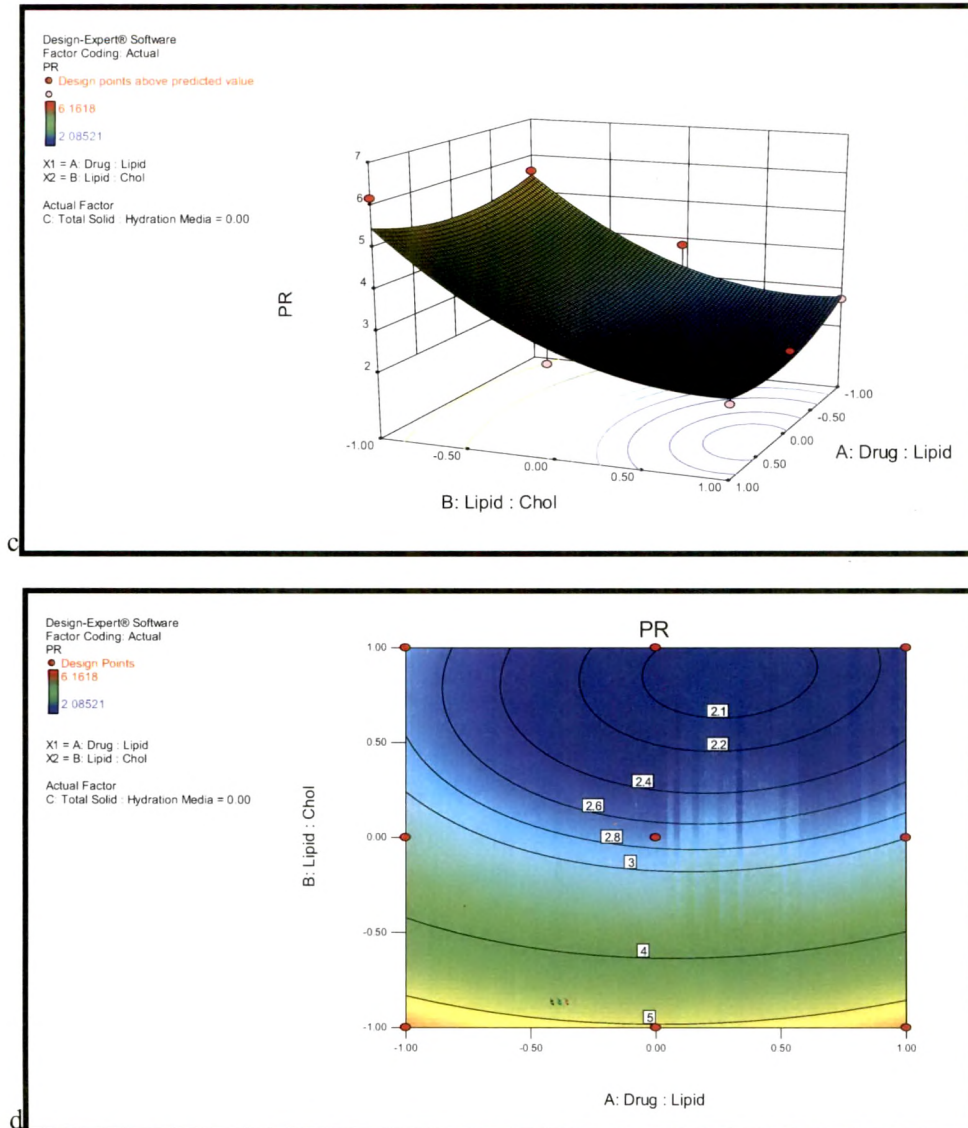
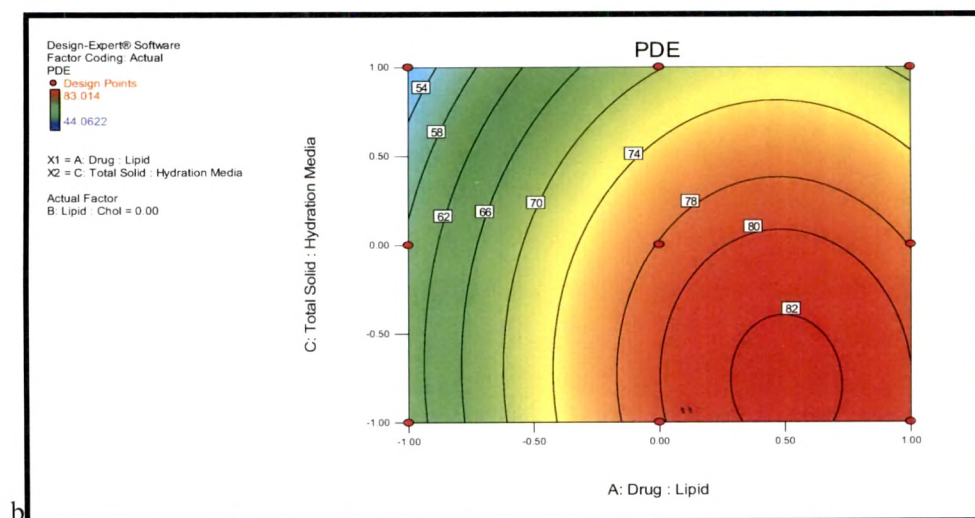
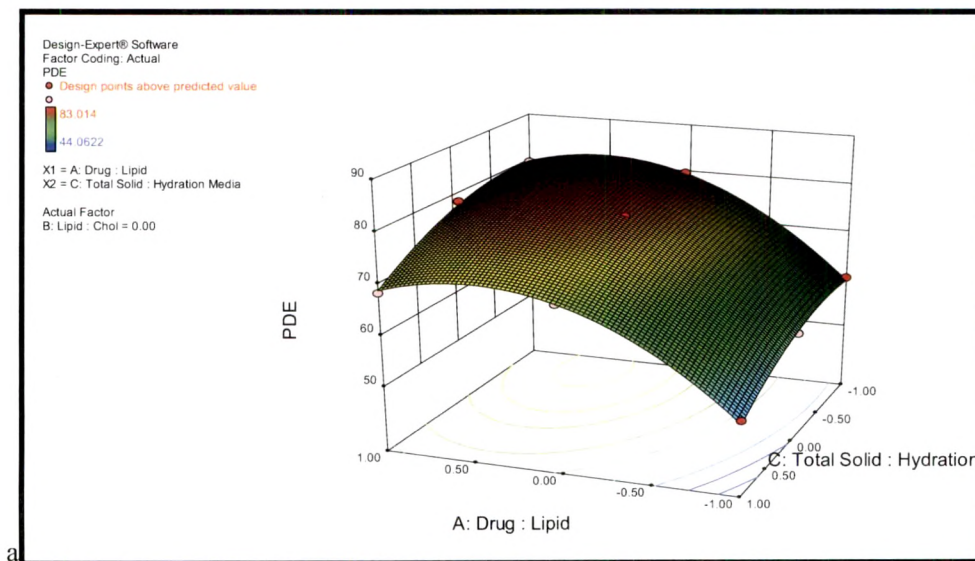


Figure 4.1 Response surface plot and corresponding contour plot showing the influence of Drug:Lipid and Lipid:Chol ratio on PDE (a & b) and PR (c & d) for RGZ



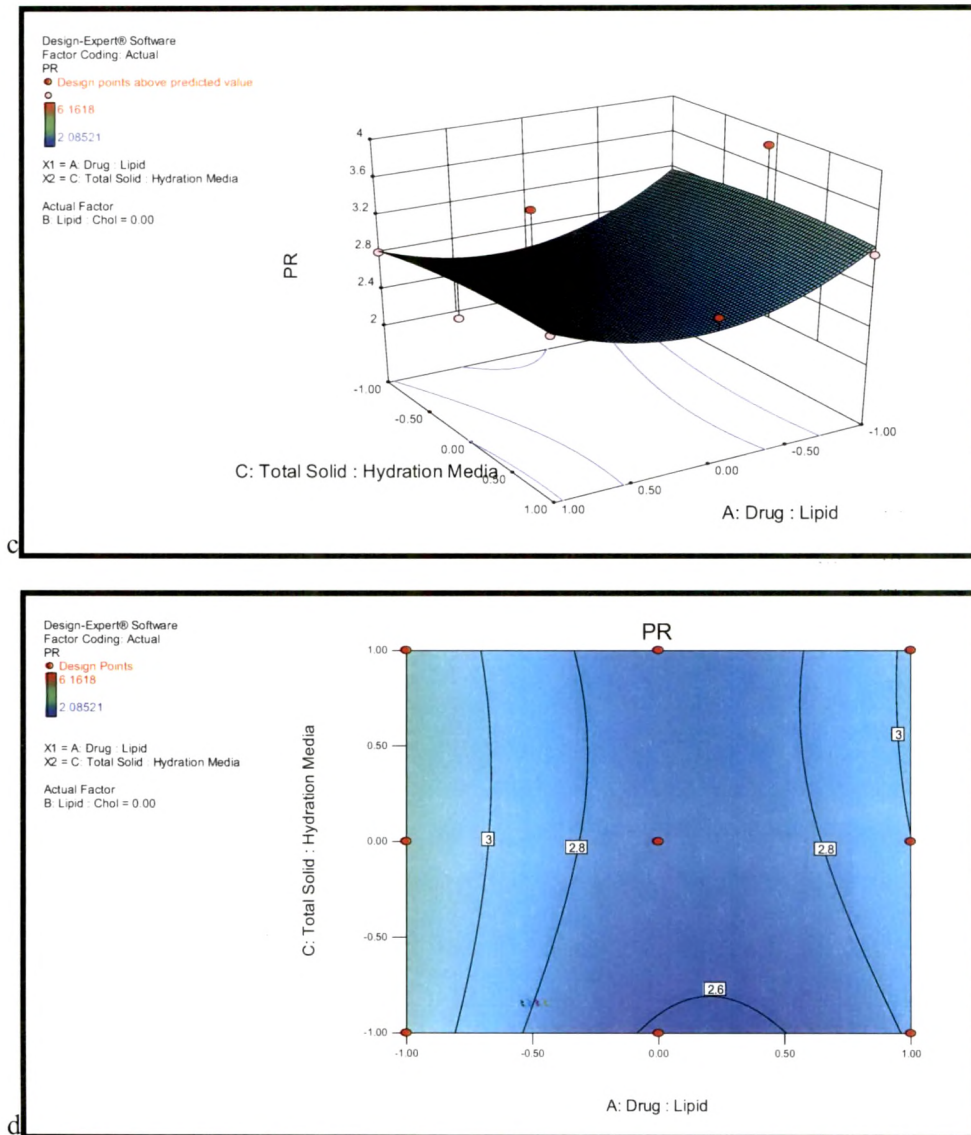
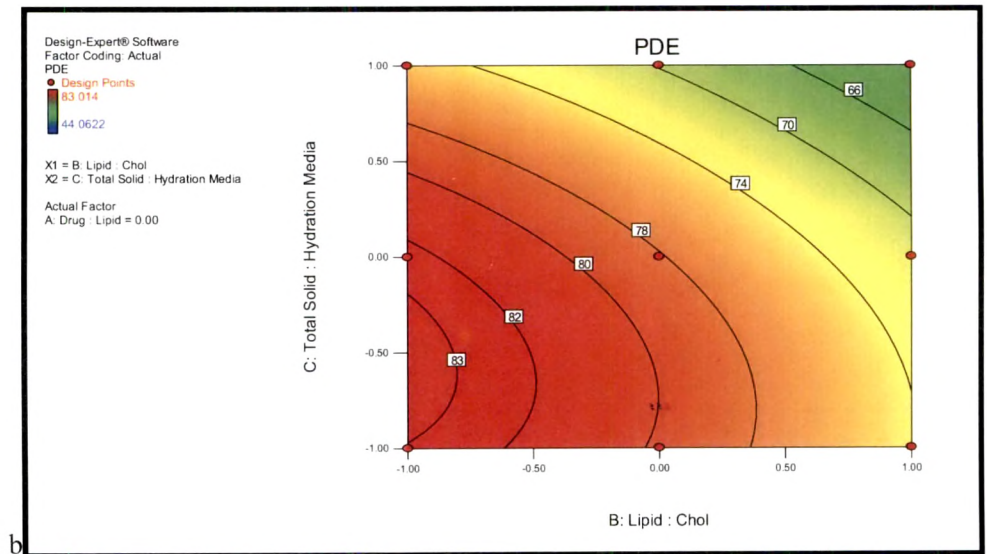
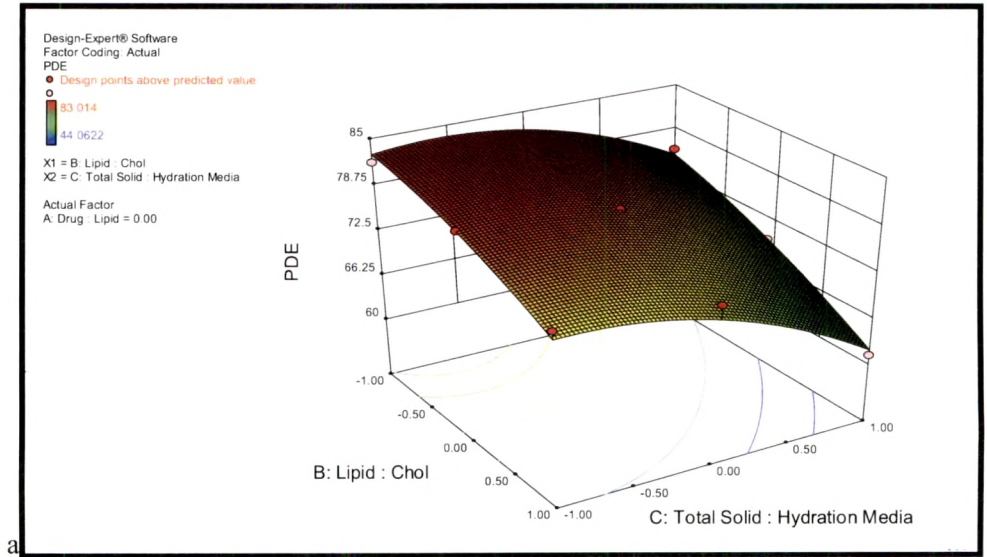


Figure 4.2 Response surface plot and corresponding contour plot showing the influence of Drug:Lipid and Total solid:Hydration medium ratio on PDE (a & b) and PR (c & d) for RGZ



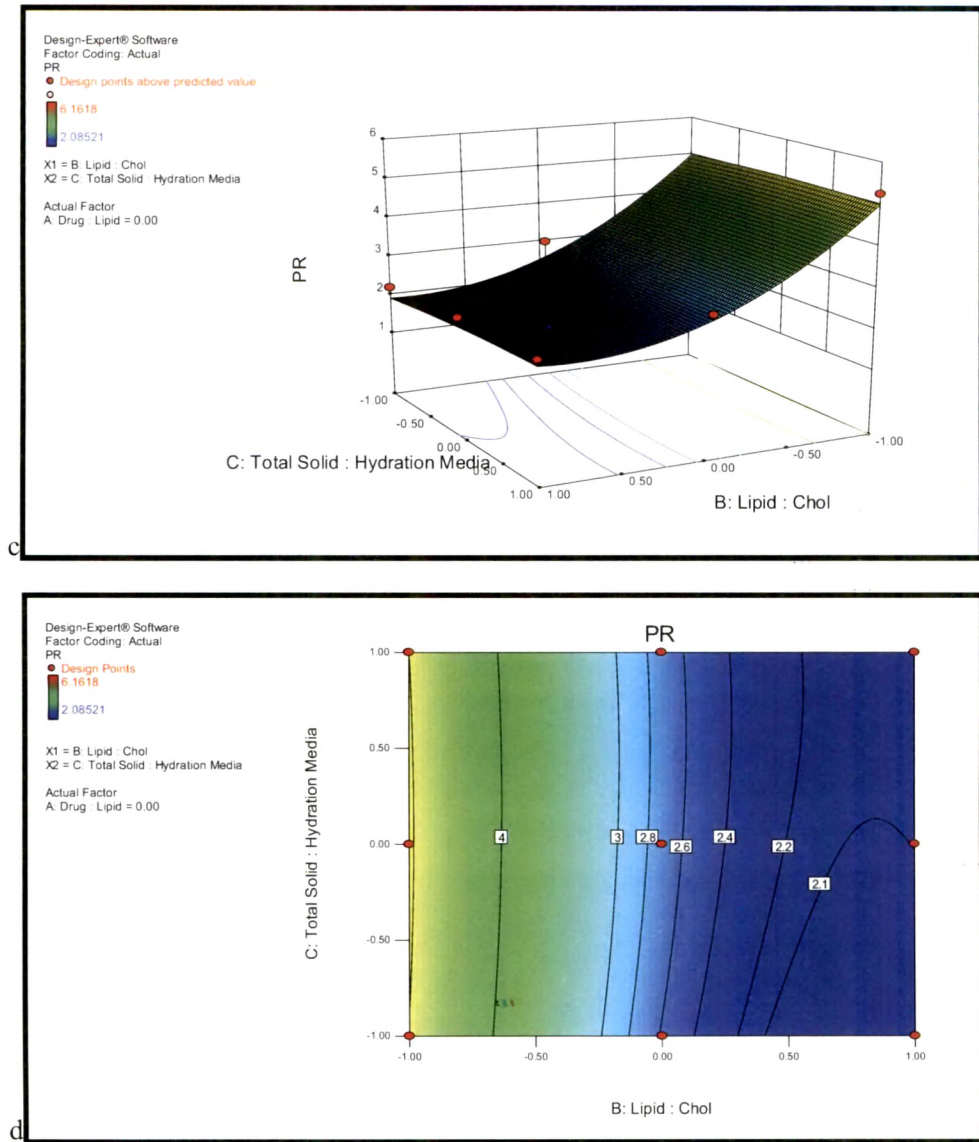


Figure 4.3 Response surface plot and corresponding contour plot showing the influence of Lipid:Chol and Total solid:Hydration medium ratio on PDE (a & b) and PR (c & d) for RGZ

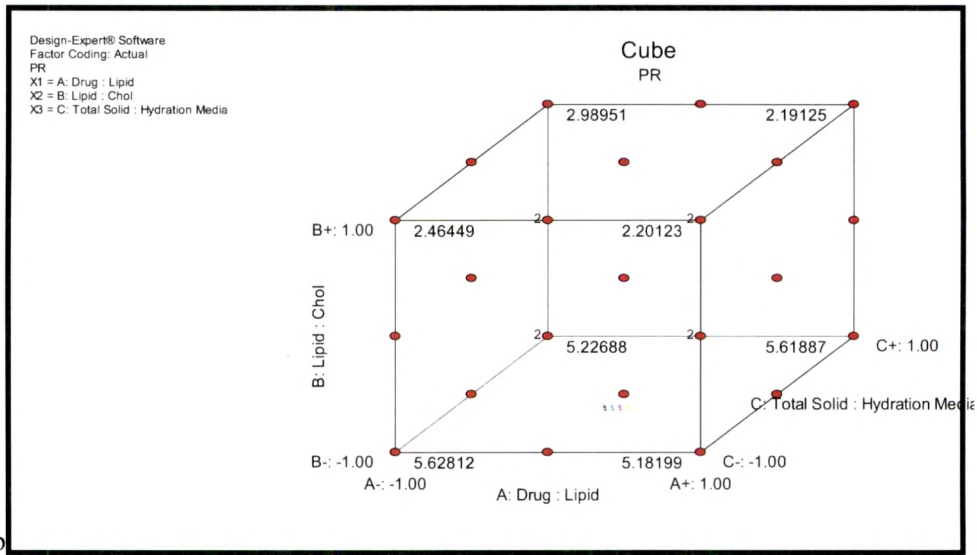
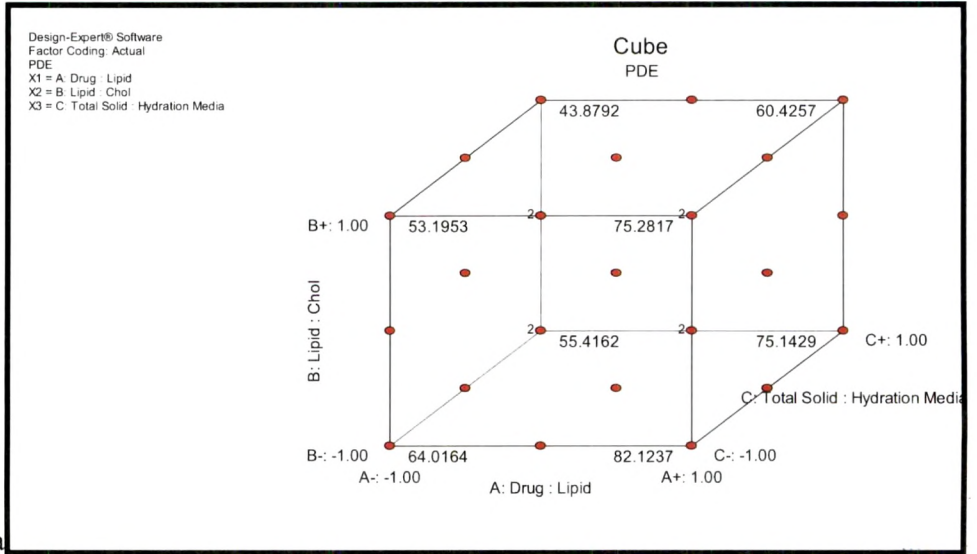


Figure 4.4 Cube plots for PDE (a) and PR (b) representing the effects of three factors at a time for RGZ

Figure 4.1a and 4.1c represent response surface plot and figure 4.1b and 4.1d correspond to contour plots showing the influence of drug:lipid and lipid:cholesterol ratio on PDE (figure 4.1a & 4.1b) and PR (figure 4.1c & 4.1d) by keeping the total solid:hydration medium ratio at 0.0. Rapid increase in PDE was observed with increase in drug:lipid ratio from -1.0 to 0.0, thereafter there was a bare minimum change in PDE and drug:lipid ratio had very little or no effect on PR. On the other

part, increase in lipid: cholesterol ratio was associated with rapid decrease in PR and had minimum effect on PDE.

Figure 4.2a and 4.2c represent response surface plot and figure 4.2b and 4.2d correspond to contour plots showing the influence of drug:lipid and total solid:hydration medium ratio on PDE (figure 4.2a & 4.2b) and PR (figure 4.2c & 4.2d) by keeping the lipid:cholesterol ratio at 0.0. Hasty increase in PDE was observed with raise in drug:lipid ratio from -1.0 to 0.0, thereafter there was a least change in PDE. Slight decrease in PR was seen with increase in drug:lipid ratio from -1.0 to 0.0 but from 0.0 to 1.0 there was a slight increase in PR. On the other side, total solid:hydration medium ratio had minimum effect on both PDE and PR.

Figure 4.3a and 4.3c represent response surface plot and figure 4.3b and 4.3d correspond to contour plots showing the influence of lipid:cholesterol and total solid:hydration medium on PDE (figure 4.3a & 4.3b) and PR (figure 4.3c & 4.3d) by keeping the drug:lipid ratio at 0.0. Slow decrease in PDE and rapid decrease in PR were observed with increase in lipid:cholesterol ratio from -1.0 to 0.0, thereafter i.e. from 0.0 to 1.0, the decrease in PDE was slightly faster and the decrease in PR was somewhat sluggish. On the other part, no change in PDE was observed with increase in total solid:hydration medium ratio from -1.0 to 0.0 thereafter, i.e. from 0.0 to 1.0, there was a decrease in PDE. Total solid:hydration medium ratio had minimum effect on PR.

Effect of all the three formulation variables on the response parameters at a time are represented in the form of cube plots in figure 4.4a (PDE) and figure 4.4b (PR).

4.10.2.1 Checkpoint Analysis

Eight checkpoint batches were prepared three times and evaluated for the results of response variables. Compositions of each checkpoint batch along with the predicted and experimental values, percentage error and p-value is listed in Table 4.6. Linear correlation plots between the observed and predicted response variables along with r^2 values are shown in figure 4.5a and 4.5b for PDE and PR respectively. P-value > 0.05 indicates the differences between predicted and experimental values are statistically insignificant. Higher r^2 values (0.9947 and 0.9995 for PDE and PR respectively) of

the linear correlation plots suggest excellent goodness of fit and high predictive capability of RSM.

Table 4.6 Checkpoint Analysis. The data represent the mean \pm SEM (n = 3).

S R N O	Formulation composition			Comparison							
	Drug:Lipid molar ratio	Lipid:Cholesterol molar ratio	Total solid content: Volume of hydration media	PDE			P value	PR			P value
				Predicted Value	Experimental value (Mean \pm SEM)	Percentage error		Predicted Value	Experimental value (Mean \pm SEM)	Percentage error	
1	-0.7 (1:16.5)	0.4 (7.6:2.4)	0.2 (13:1)	63.11	64.12 \pm 0.972	1.596	P > 0.05 Non significant	2.62	2.58 \pm 0.035	-1.400	P > 0.05 Non significant
2	-0.4 (1:18)	0.2 (7.8:2.2)	-0.3 (11.75:1)	72.76	71.64 \pm 1.006	1.539		2.56	2.57 \pm 0.047	0.521	
3	0.9 (1:24.5)	-0.3 (8.3:1.7)	0.6 (14:1)	76.16	75.31 \pm 1.083	1.116		3.54	3.49 \pm 0.052	-1.506	
4	0.7 (1:23.5)	-0.5 (8.5:1.5)	-0.5 (11.25:1)	83.8	82.56 \pm 1.038	1.476		3.74	3.68 \pm 0.055	-1.604	
5	0.2 (1:21)	-0.8 (8.8:1.2)	0.5 (13.75:1)	80.36	79.15 \pm 1.040	1.506		4.47	4.39 \pm 0.064	-1.715	
6	-0.3 (1:18.5)	0.8 (7.2:2.8)	-0.8 (10.5:1)	71.4	69.58 \pm 1.026	2.545		2.04	2.00 \pm 0.038	-1.961	
7	-0.9 (1:15.5)	0.9 (7.1:2.9)	0.8 (14.5:1)	49.56	48.67 \pm 0.970	1.796		2.8	2.74 \pm 0.041	-2.024	
8	-0.8 (1:16)	-0.7 (8.7:1.3)	-0.6 (11:1)	68.87	68.07 \pm 0.873	1.157		4.52	4.45 \pm 0.064	-1.622	

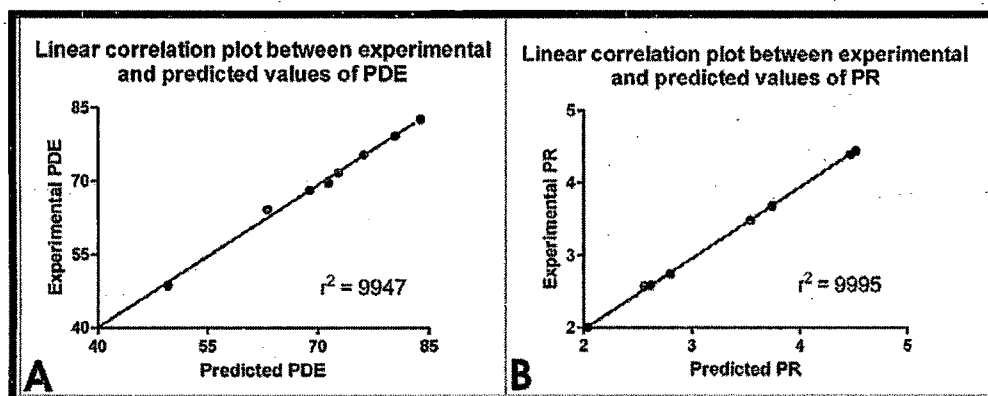


Figure 4.5 Linear correlation plots of the experimental response values versus the predicted response values for PDE (a) and PR (b) for RGZ

The optimum formulation was derived by deciding goals for each formulation variable and response parameter and allotting the importance to each of them. By fixing the goal and importance we derived an optimum formulation as described in Table 4.7. The optimized batch (Drug: Lipid molar ratio = -0.02; Lipid: Cholesterol molar ratio = 0.40; Total solid content: Volume of hydration media = 0.02) was actually prepared and the experimental results were compared with predicted values.

P-value > 0.05 indicates the differences between predicted and experimental values are statistically insignificant.

Table 4.7 Derivation of optimized formulation. The data represent the mean \pm SEM (n = 3).

Constrains			Lower Limit	Upper Limit	Predicted solution [A]	Actual results (Mean \pm SEM) [B]	Comparison of A and B (P value)
Name	Goal	Importance					
Drug:Lipid molar ratio	Minimize	5	-1	1	-0.20	-0.02	
Lipid:Cholesterol molar ratio	Maximize	2	-1	1	0.40	0.40	
Total solid content: Volume of hydration media	Minimize	2	-1	1	0.02	0.02	
PDE	Maximize	5	44.062	83.014	73.32	71.83 \pm 0.683	P > 0.05, Non significant
PR	Minimize	2	2.0852	6.1618	2.32	2.41 \pm 0.081	P > 0.05 Non significant

4.10.3 Formulation Optimization CDS Loaded Liposomes Using Response Surface Methodology (RSM)

All twenty seven batches of liposomes were prepared according to the formulation variables as shown in Table 4.8. All formulations were evaluated for PDE and PR and the results obtained are shown in Table 4.8.

Table 4.8 3³ Full factorial design outline with results for PDE and PR. The data represent the mean ± SEM (n = 3).

Batch No.	X1	X2	X3	X1 ²	X2 ²	X3 ²	X1X2	X2X3	X1X3	X1X2X3	PDE (mean* ± SEM)	PR (mean* ± SEM)
1	0	0	-1	0	0	1	0	0	0	0	71.53 ± 0.994	3.06 ± 0.063
2	0	0	0	0	0	0	0	0	0	0	70.28 ± 1.021	3.00 ± 0.074
3	0	0	1	0	0	1	0	0	0	0	61.64 ± 0.857	3.77 ± 0.068
4	0	-1	-1	0	1	1	0	1	0	0	74.17 ± 1.113	4.95 ± 0.089
5	0	-1	0	0	1	0	0	0	0	0	72.57 ± 0.991	5.34 ± 0.097
6	0	-1	1	0	1	1	0	-1	0	0	66.28 ± 0.894	5.81 ± 0.121
7	0	1	-1	0	1	1	0	-1	0	0	65.97 ± 0.786	2.72 ± 0.059
8	0	1	0	0	1	0	0	0	0	0	64.37 ± 0.954	2.91 ± 0.068
9	0	1	1	0	1	1	0	1	0	0	52.49 ± 0.584	2.64 ± 0.062
10	-1	0	-1	1	0	1	0	0	1	0	51.68 ± 0.701	3.26 ± 0.093
11	-1	0	0	1	0	0	0	0	0	0	49.96 ± 0.723	3.65 ± 0.105
12	-1	0	1	1	0	1	0	0	-1	0	43.94 ± 0.631	3.76 ± 0.091
13	-1	-1	-1	1	1	1	1	1	1	-1	56.58 ± 0.711	5.82 ± 0.118
14	-1	-1	0	1	1	0	1	0	0	0	54.85 ± 0.672	5.94 ± 0.133
15	-1	-1	1	1	1	1	1	-1	-1	1	45.48 ± 0.559	5.92 ± 0.108
16	-1	1	-1	1	1	1	-1	-1	1	1	42.82 ± 0.598	2.69 ± 0.073
17	-1	1	0	1	1	0	-1	0	0	0	40.52 ± 0.635	3.17 ± 0.072
18	-1	1	1	1	1	1	-1	1	-1	-1	36.41 ± 0.526	3.26 ± 0.081
19	1	0	-1	1	0	1	0	0	-1	0	71.20 ± 0.739	3.00 ± 0.066
20	1	0	0	1	0	0	0	0	0	0	69.65 ± 0.971	3.02 ± 0.068
21	1	0	1	1	0	1	0	0	1	0	61.10 ± 0.877	3.45 ± 0.075
22	1	-1	-1	1	1	1	-1	1	-1	1	73.93 ± 0.955	5.78 ± 0.119
23	1	-1	0	1	1	0	-1	0	0	0	72.42 ± 0.911	5.90 ± 0.120
24	1	-1	1	1	1	1	-1	-1	1	-1	66.56 ± 0.858	5.75 ± 0.114
25	1	1	-1	1	1	1	1	-1	-1	-1	65.82 ± 1.042	2.04 ± 0.059
26	1	1	0	1	1	0	1	0	0	0	63.19 ± 0.793	2.11 ± 0.054
27	1	1	1	1	1	1	1	1	1	1	51.79 ± 0.667	2.32 ± 0.066

A full model for both PDE and PR was established by putting the values of intercepts and regression coefficients in polynomial equation.

PDE Full equation

$$Y_{PDE} = 69.99638 + 9.633683 X_1 - 5.52636 X_2 - 4.88825 X_3 - 10.0405 X_1^2 - 1.98564 X_2^2 - 3.12295 X_3^2 + 0.420818 X_1X_2 - 0.63064 X_2X_3 - 0.52058 X_1X_3 - 1.41881 X_1X_2X_3$$

PR Full equation

$$Y_{PR} = 3.24391 - 0.22759 X_1 - 1.51856 X_2 + 0.18723 X_3 + 0.13591 X_1^2 + 0.83919 X_2^2 - 0.00416 X_3^2 - 0.19882 X_1X_2 - 0.01364 X_2X_3 - 0.03916 X_1X_3 - 0.01992 X_1X_2X_3$$

The Model F-value of 311.861 and 71.205 respectively for PDE and PR implies the model is significant. For both PDE and PR, there is only a 0.01% chance that a "Model F-Value" this large could occur due to noise. Values of "Probability value > F" less than 0.0500 indicate model terms are significant. In the case of PDE X₁, X₂,

X_3 , X_1^2 , X_2^2 , X_3^2 and $X_1X_2X_3$ and in the case of PR X_1 , X_2 , X_3 , X_2^2 and X_1X_2 are significant model terms. Values greater than 0.1000 indicate the model terms are not significant. If there are many insignificant model terms model reduction may improve the model.

PDE Reduced equation

$$Y_{PDE} = 69.99638 + 9.633683 X_1 - 5.52636 X_2 - 4.88825 X_3 - 10.0405 X_1^2 - 1.98564 X_2^2 - 3.12295 X_3^2 - 1.41881 X_1X_2X_3$$

PR Reduced equation

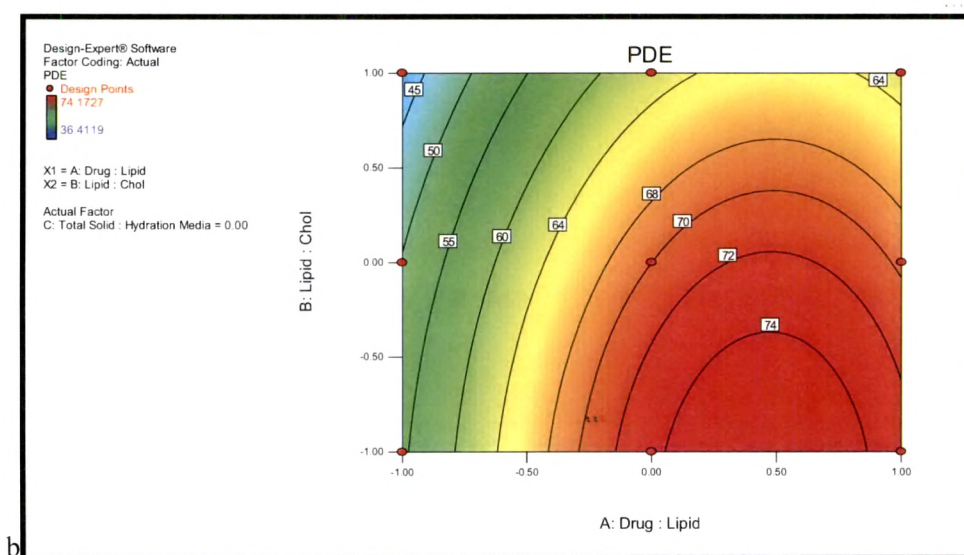
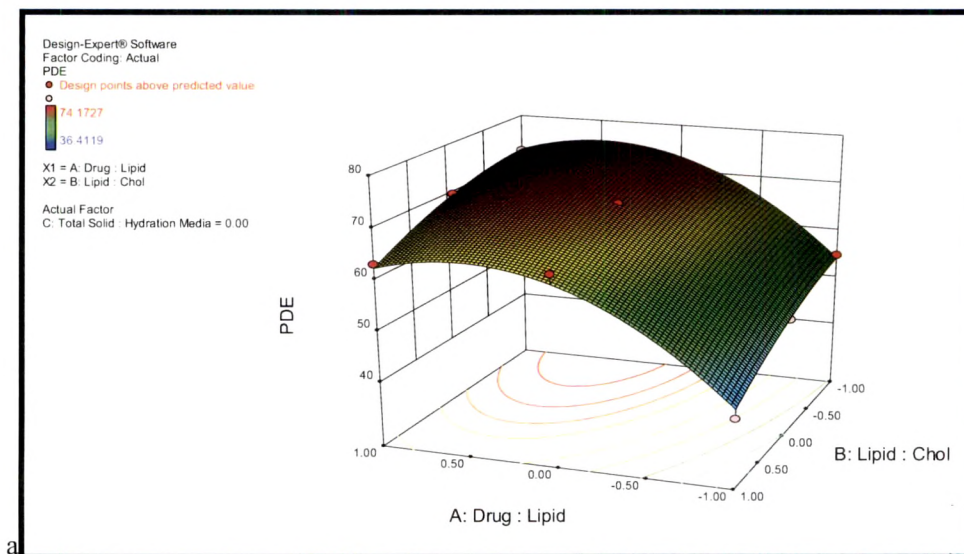
$$Y_{PR} = 3.33174 - 0.2276 X_1 - 1.51856 X_2 + 0.18723 X_3 + 0.83919 X_2^2 - 0.19882 X_1X_2$$

The "Predicted R-Squared" of 0.9843 is in reasonable agreement with the "Adjusted R-Squared" of 0.9917 in case of PDE and the "Predicted R-Squared" of 0.9286 is in reasonable agreement with the "Adjusted R-Squared" of 0.9643 in the case of PE. "Adequate Precision" measures the signal to noise ratio. A ratio greater than 4 is desirable. The ratio of 58.81 for PDE and 23.12 for PR indicates an adequate signal. This model can be used to navigate the design space.

Comparison of full model (FM) and reduced model (RM) was done by analysis of variance (ANOVA) by applying the F-Statistic to check effect of omission of the statistically insignificant coefficients from the full model and the results are shown in Table 4.9.

Table 4.9 Analysis of Variance (ANOVA) of full and reduced models

Response	Model		df	SS	MS	F	Adjusted R ²	Predicted R ²	ANOVA comparison	
									F Calculated	F Tabulated
PDE	Regression	FM	10	3363.677	336.368	311.861	0.9917	0.9843	3.1367	3.24
		RM	8	3353.527	479.075	332.122				
	Residual (Error)	FM	16	17.257	1.079					
		RM	18	27.407	1.443					
PE	Regression	FM	10	47.906	4.791	71.205	0.9643	0.9286	0.4005	2.85
		RM	3	43.182	10.796	40.947				
	Residual (Error)	FM	16	1.076	0.067					
		RM	23	5.800	0.264					



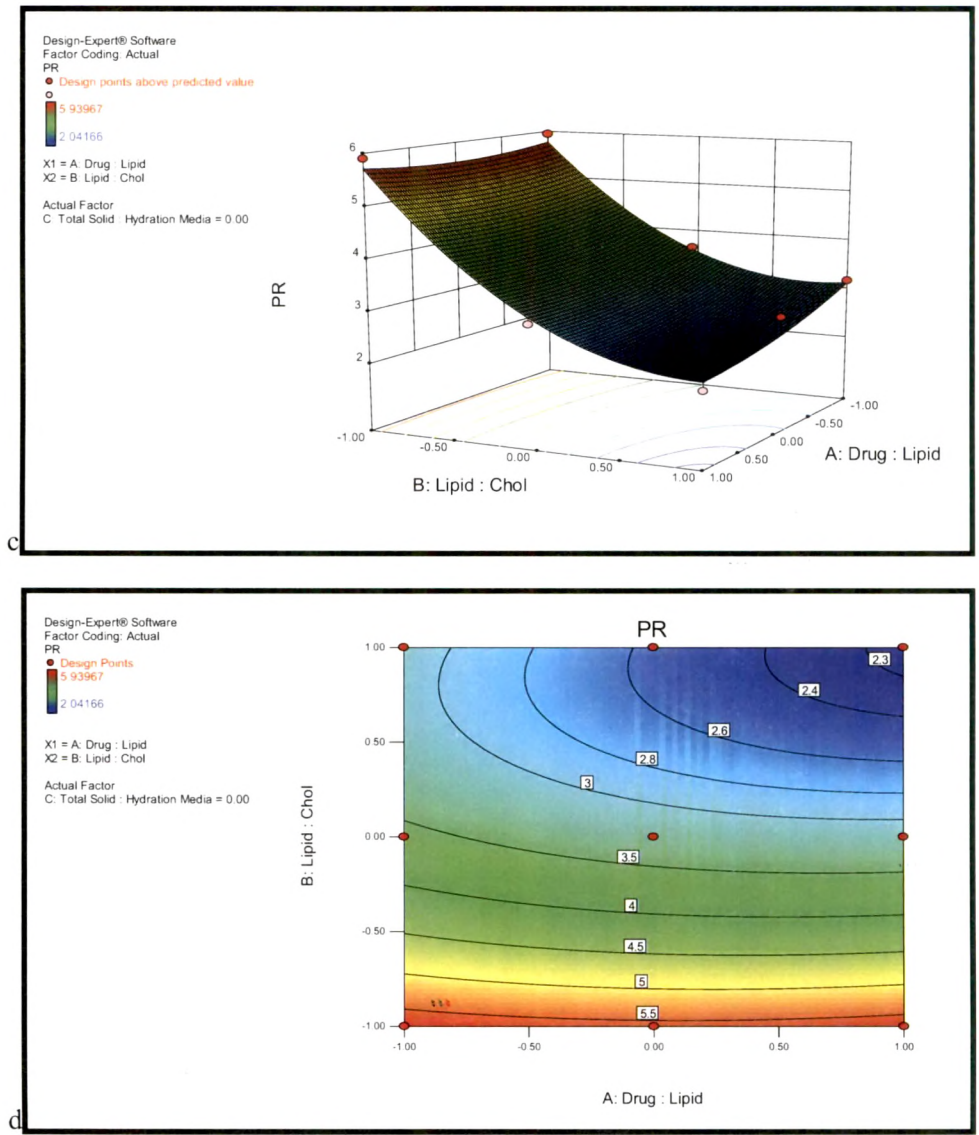
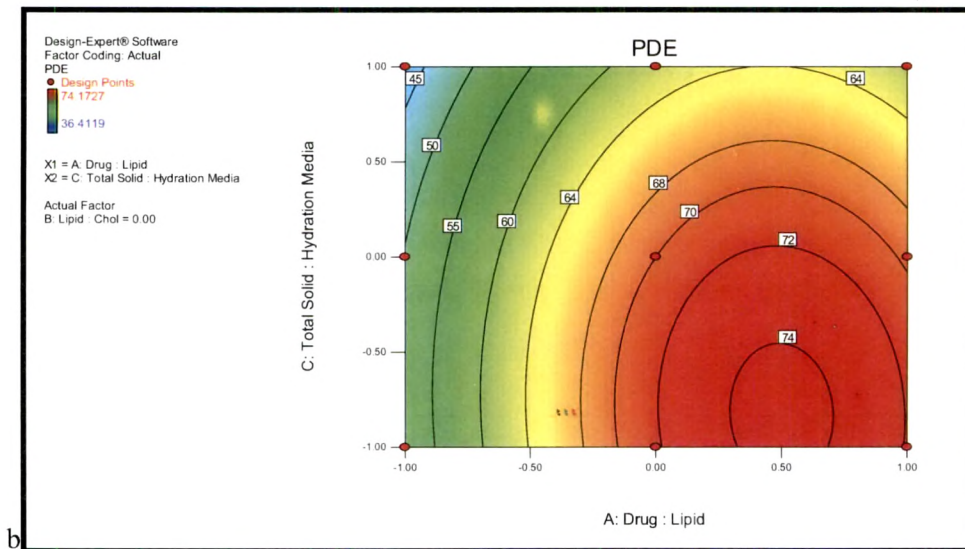
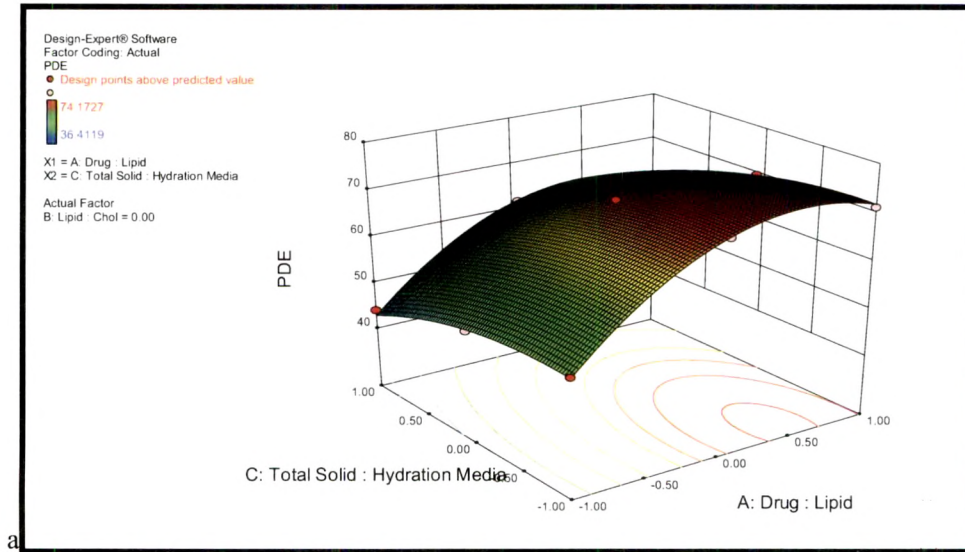


Figure 4.6 Response surface plot and corresponding contour plot showing the influence of Drug: Lipid and Lipid: Chol ratio on PDE (a & b) and PR (c & d) for CDS



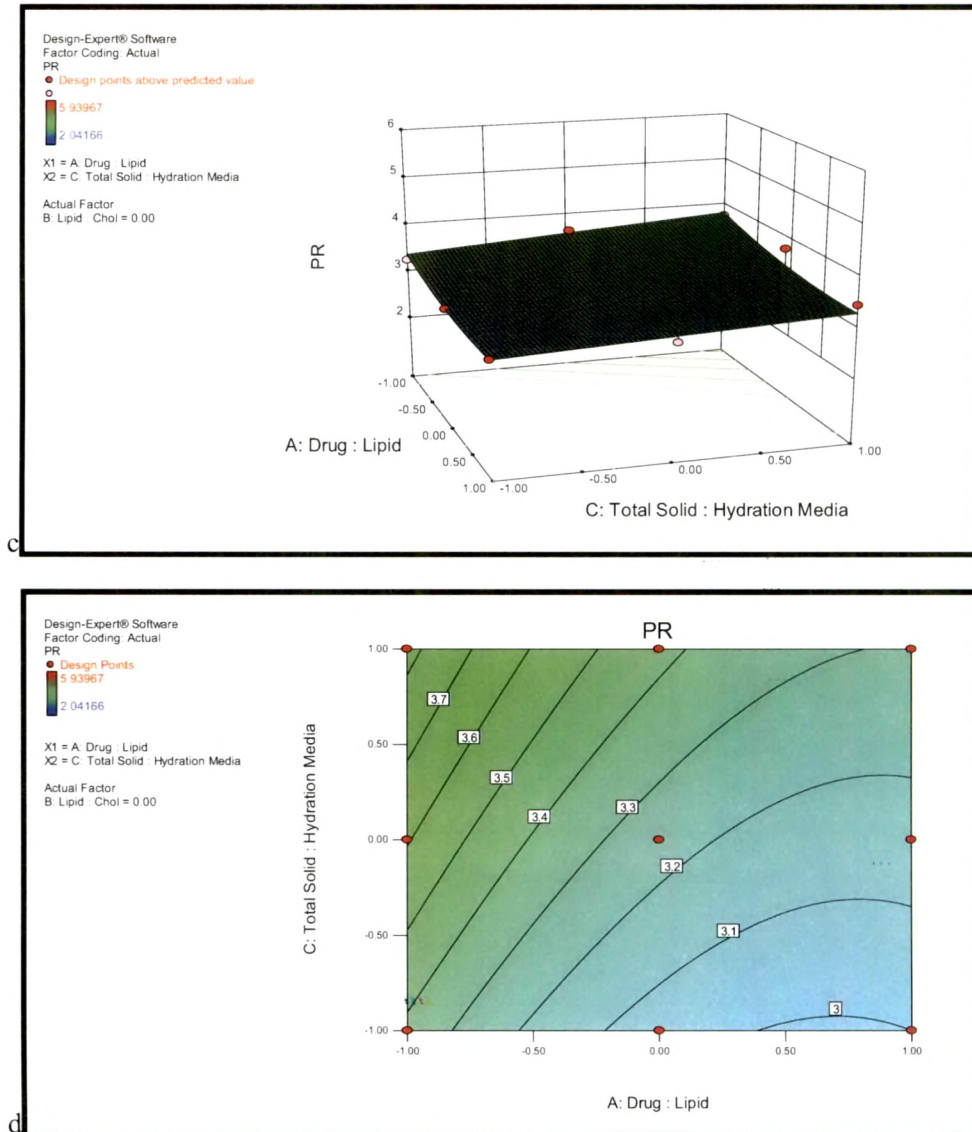
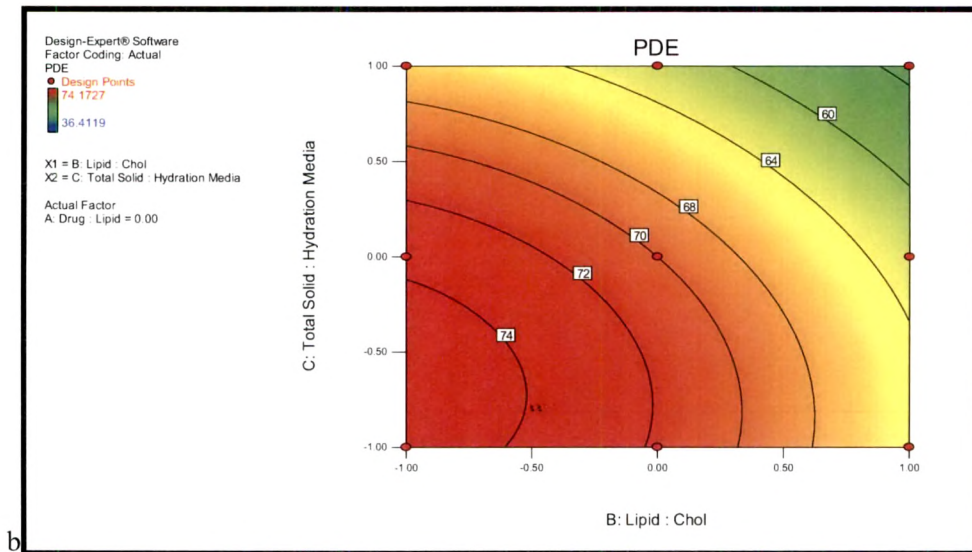
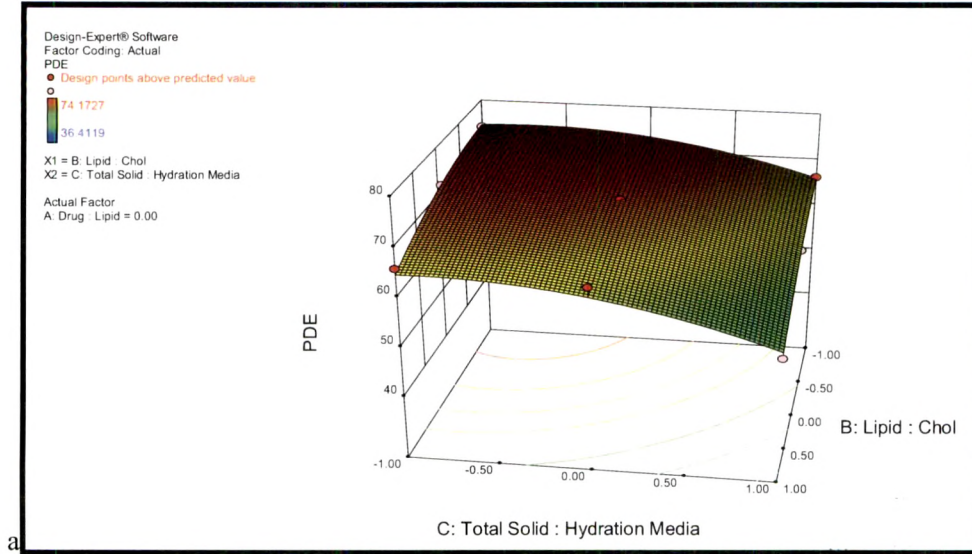


Figure 4.7 Response surface plot and corresponding contour plot showing the influence of Drug: Lipid and Total solid: Hydration medium ratio on PDE (a & b) and PR (c & d) for CDS



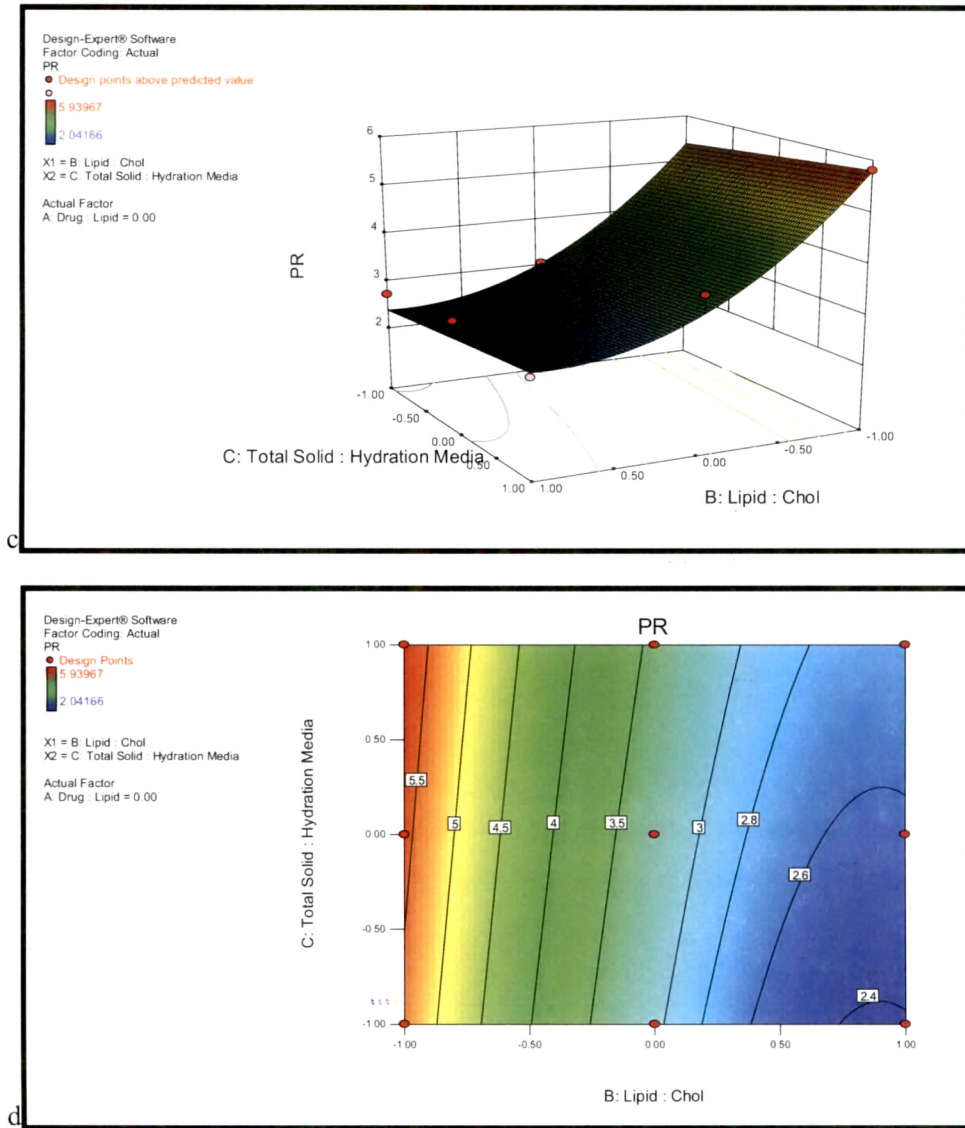


Figure 4.8 Response surface plot and corresponding contour plot showing the influence of Lipid: Chol and Total solid: Hydration medium ratio on PDE (a & b) and PR (c & d) for CDS

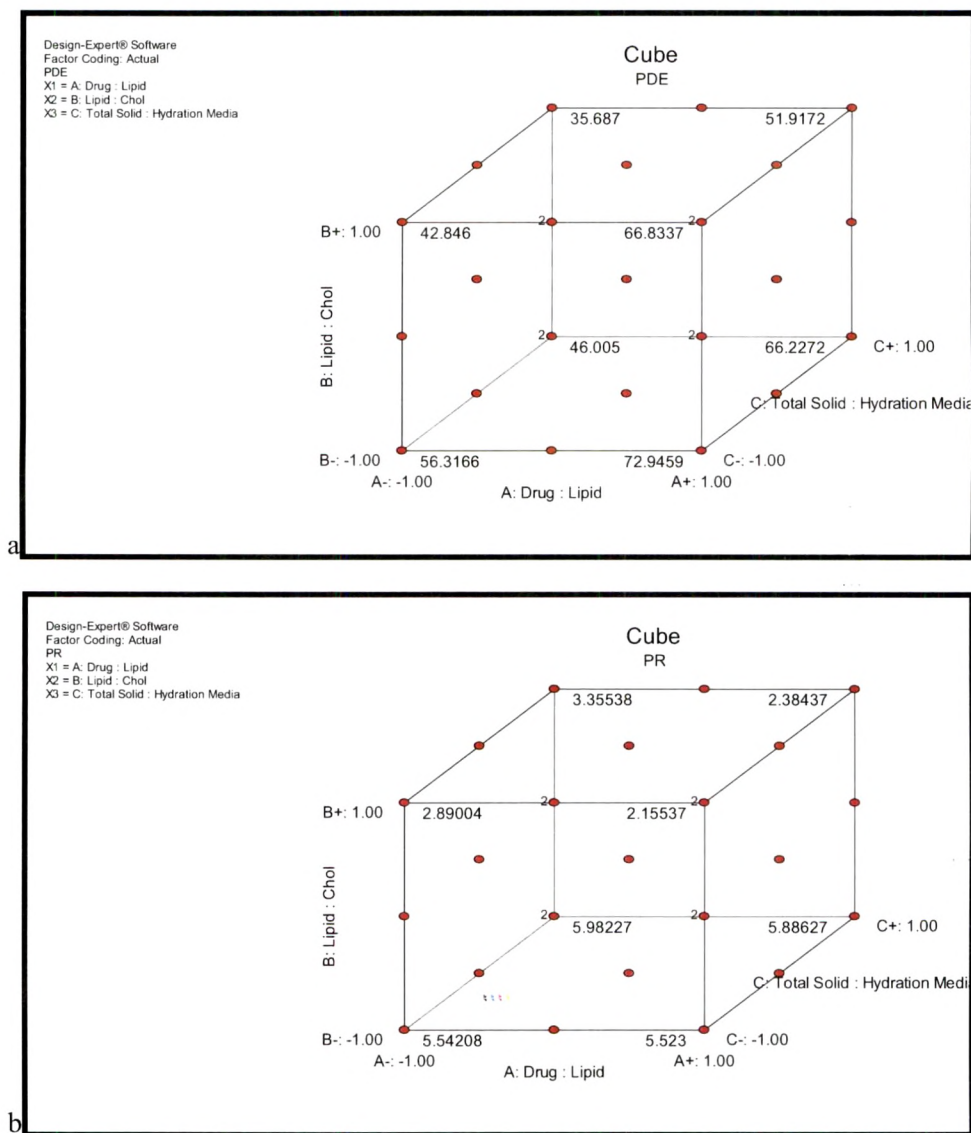


Figure 4.9 Cube plots for PDE (a) and PR (b) representing the effects of three factors at a time for CDS

Figure 4.6a and 4.6c represent response surface plot and figure 4.6b and 4.6d correspond to contour plots showing the influence of drug: lipid and lipid: cholesterol ratio on PDE (4.6a & 4.6b) and PR (4.6c & 4.6d) by keeping the total solid: hydration medium ratio at 0.0. Rapid increase in PDE was observed with increase in drug: lipid ratio from -1.0 to 0.0 then after there was a bare minimum change in PDE and drug: lipid ratio had very little or no effect on PR. On the other part, increase in lipid:

cholesterol ratio was associated with rapid decrease in PR and had minimum effect on PDE.

Figure 4.7a and 4.7c represent response surface plot and figure 4.7b and 4.7d correspond to contour plots showing the influence of drug: lipid and total solid: hydration medium ratio on PDE (4.7a & 4.7b) and PR (4.7c & 4.7d) by keeping the lipid: cholesterol ratio at 0.0. Hasty increase in PDE was observed with raise in drug: lipid ratio from -1.0 to 0.0 then after there was a least change in PDE. Slight decrease in PR was seen with increase in drug: lipid ration from -1.0 to 1.0. On the other side, total solid: hydration medium ratio had minimum effect on PDE and very slight increase in PR is observed with increase in total solid: hydration medium ratio.

Figure 4.8a and 4.8c represent response surface plot and figure 4.8b and 4.8d correspond to contour plots showing the influence of lipid: cholesterol and total solid: hydration medium on PDE (4.8a & 4.8b) and PR (4.8c & 4.8d) by keeping the drug: lipid ratio at 0.0. Slow decrease in PDE and rapid decrease in PR were observed with increase in lipid: cholesterol ratio from -1.0 to 0.0 then after, i.e. from 0.0 to 1.0, the decrease in PDE was slightly faster and the decrease in PR was somewhat sluggish. On the other part, no change in PDE was observed with increase in total solid: hydration medium ratio from -1.0 to 0.0 then after, i.e. from 0.0 to 1.0, there was a decrease in PDE. Total solid: hydration medium ratio had minimum effect on PR.

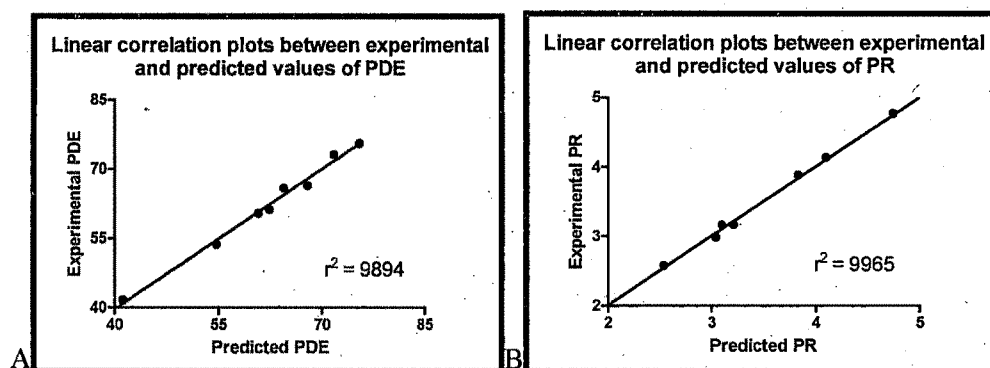
Effect of all the three formulation variables on the response parameters at a time are represented in the form of cube plots in figure 4.9a (PDE) and figure 4.9b (PR).

4.10.3.1 Checkpoint Analysis

Eight checkpoint batches were prepared three times and evaluated for the results of response variables. Compositions of each checkpoint batch along with the predicted and experimental values, percentage error and p-value is listed in Table 4.10. Linear correlation plots between the observed and predicted response variables along with r^2 values are shown in figure 4.10a and 4.10b for PDE and PR respectively. P-value > 0.05 indicates the differences between predicted and experimental values are statistically insignificant. Higher r^2 values (0.9894 and 0.9965 for PDE and PR respectively) of the linear correlation plots suggest excellent goodness of fit and high predictive capability of RSM.

Table 10 Checkpoint Analysis. The data represent the mean \pm SEM (n = 3).

S r. N o.	Formulation composition			Comparison							
	Drug: Lipid molar ratio	Lipid: Choleste rol molar ratio	Total solid content: Volume of hydratio n media	PDE			P value	PR			P value
				Predi cted Valu e	Experim ental value (Mean* \pm SEM)	Percen tage error		Predi cted Valu e	Experim ental value (Mean* \pm SEM)	Percen tage error	
1	-0.7 (1:16.5)	0.4 (7.6:2.4)	0.2 (13:1)	54.69	53.68 \pm 0.806	-1.847	P > 0.05 Non signif icant	3.10	3.16 \pm 0.057	1.936	P > 0.05 Non- signific ant
2	-0.4 (1:18)	0.2 (7.8:2.2)	-0.3 (11.75:1)	64.45	65.87 \pm 0.593	2.203		3.04	2.99 \pm 0.058	-1.645	
3	0.9 (1:24.5)	-0.3 (8.3:1.7)	0.6 (14:1)	67.91	66.44 \pm 0.394	-2.165		3.83	3.89 \pm 0.055	1.567	
4	0.7 (1:23.5)	-0.5 (8.5:1.5)	-0.5 (11.25:1)	75.38	75.56 \pm 0.390	0.239		4.10	4.14 \pm 0.069	0.976	
5	0.2 (1:21)	-0.8 (8.8:1.2)	0.5 (13.75:1)	71.69	73.15 \pm 0.546	2.037		5.08	5.01 \pm 0.074	-1.378	
6	-0.3 (1:18.5)	0.8 (7.2:2.8)	-0.8 (10.5:1)	62.33	61.25 \pm 0.709	-1.733		2.54	2.58 \pm 0.055	1.575	
7	-0.9 (1:15.5)	0.9 (7.1:2.9)	0.8 (14.5:1)	41.20	41.67 \pm 0.711	1.141		3.21	3.17 \pm 0.062	-1.246	
8	-0.8 (1:16)	-0.7 (8.7:1.3)	-0.6 (11:1)	60.77	60.41 \pm 0.607	-0.592		4.74	4.77 \pm 0.059	0.633	

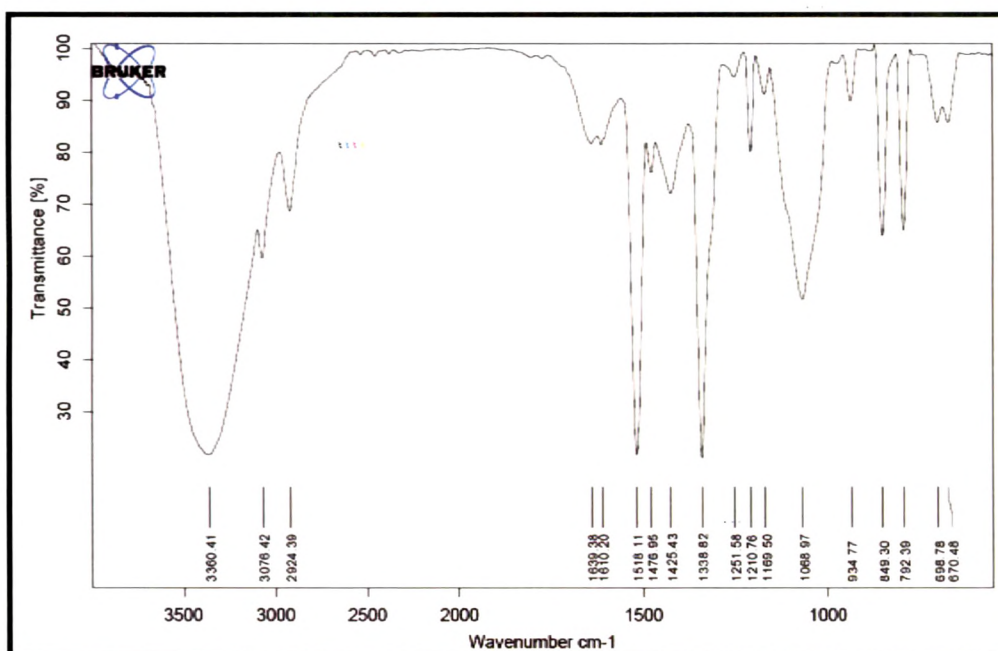

Figure 4.10 Linear correlation plots of the experimental response values versus the predicted response values for PDE (a) and PR (b) for CDS

The optimum formulation was derived by deciding goals for each formulation variable and response parameter and allotting the importance to each of them. By fixing the goal and importance we derived an optimum formulation as described in Table 4.11. The optimized batch (Drug: Lipid molar ratio = -0.35; Lipid: Cholesterol molar ratio = 0.60; Total solid content: Volume of hydration media = -1.00) was actually prepared and the experimental results were compared with predicted values. P-value > 0.05 indicates the differences between predicted and experimental values are statistically insignificant.

Table 4.11 Derivation of optimized formulation. The data represent the mean \pm SEM (n = 3).

Constrains			Lower Limit	Upper Limit	Predicted solution [A]	Actual results (Mean \pm SEM) [B]	Comparison of A and B (P value)
Name	Goal	Importance					
Drug: Lipid molar ratio	Minimize	5	-1	1	-0.35	-0.35	
Lipid: Cholesterol molar ratio	Maximize	2	-1	1	0.60	0.60	
Total solid content: Volume of hydration media	Minimize	2	-1	1	-1.00	-1.00	
PDE	Maximize	5	36.412	74.173	62.879	64.01 \pm 0.772	P > 0.05, Non significant
PR	Minimize	2	2.042	5.940	2.570	2.481 \pm 0.076	P > 0.05 Non significant

4.10.4 Preparation of M6P-HSA


Figure 4.11 IR spectra of p-nitrophenyl-a-D-mannopyranoside

In FTIR spectroscopy (BRUKER, α -Alpha T, Germany) presence of strong peaks at 2345.56 and 941.88 and a broad peak at 1708.14 confirms presence of (O=P-OH) group and strong peak at 2850.47 confirms presence of (P-O-H) group (figure 4.12).

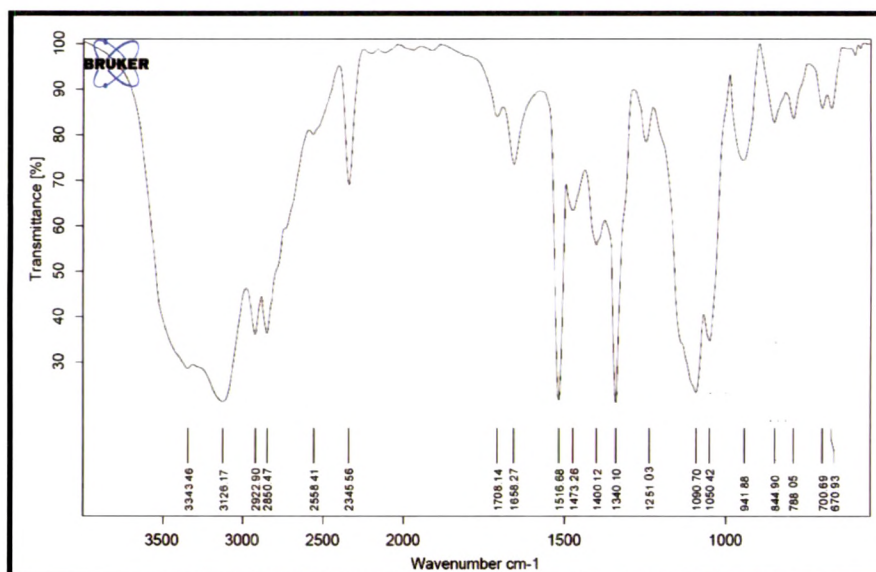


Figure 4.12 IR spectra of p-nitrophenyl-6-phospho- α -D-mannopyranoside

Presence of weak peaks at 3510.31 and 3420.28 and a medium peak at 1616.28 confirms presence of (N-H) group. Absence of peaks at 1516.68 and 1340.10 confirms conversion of (NO₂) group to (NH₂) group (figure 4.13).

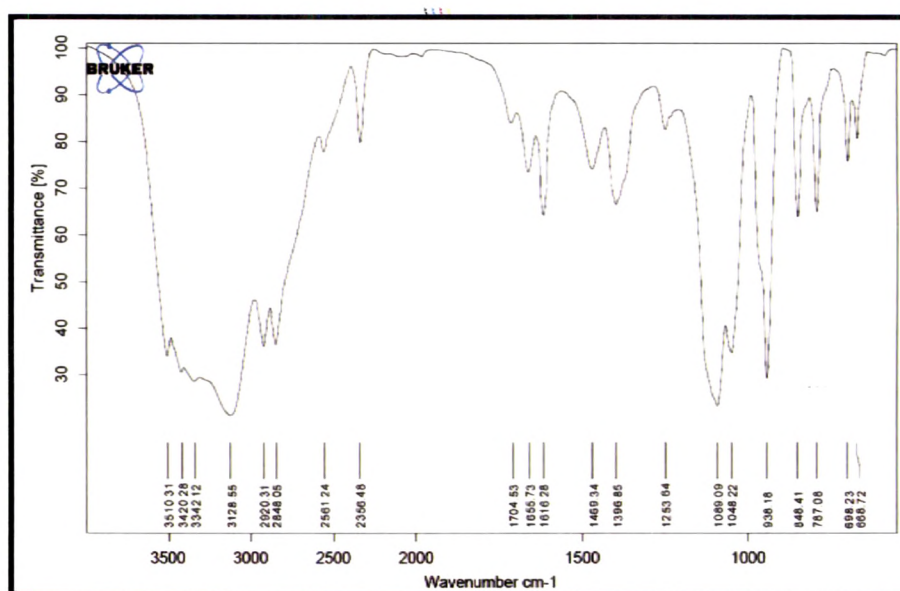


Figure 4.13 IR spectra of p-aminophenyl-6-phospho- α -D-mannopyranoside

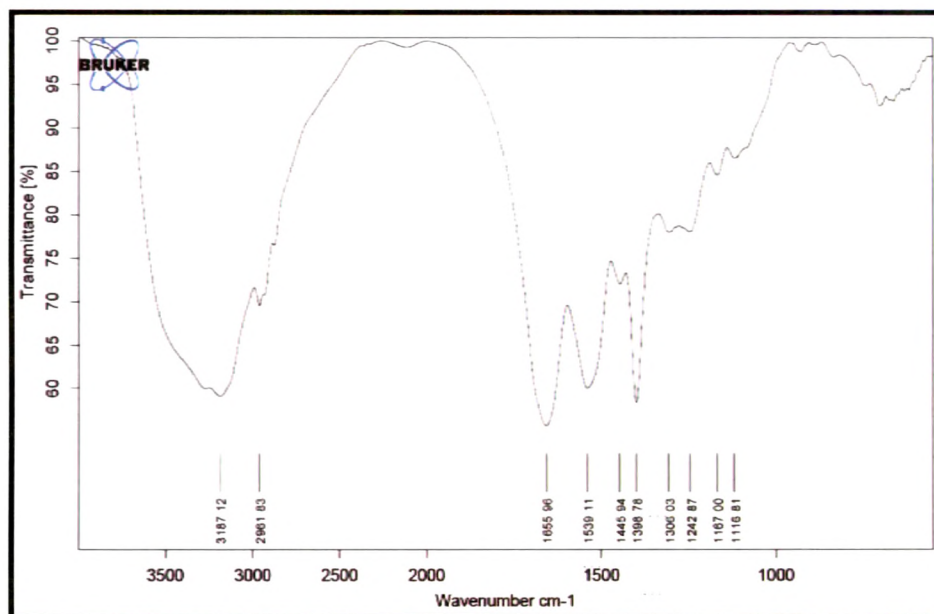


Figure 4.14 IR spectra of HSA

Presence of peak at 1575.32 confirms presence of (-N=N-) group (figure 4.15).

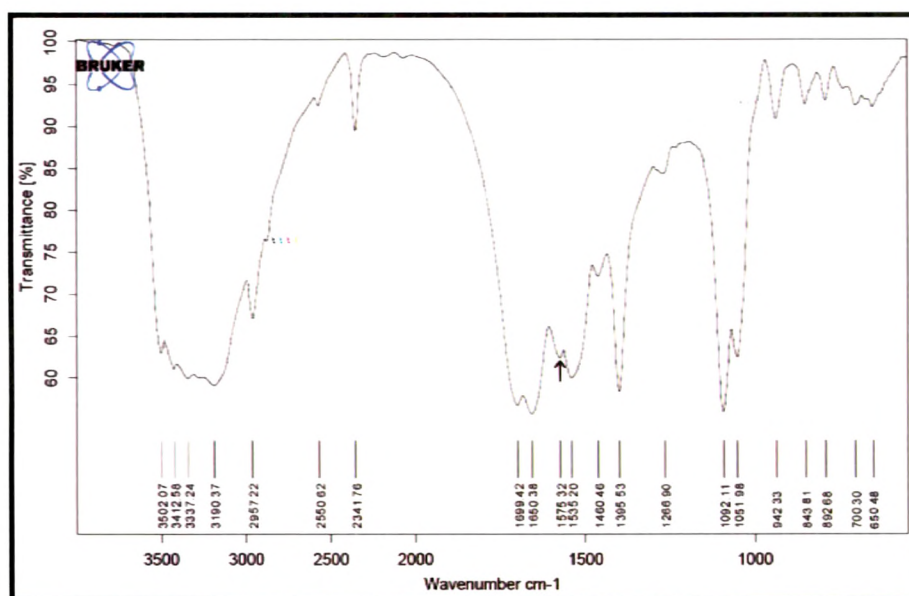


Figure 4.15 IR spectra of M6P-HSA

Prepared M6P-HSA was purified, characterized for protein content, number of M6P molecules and number of phosphate groups coupled to each HSA molecules. The prepared neoglycoprotein had $95.22 \pm 1.74\%$ of protein, 29.73 ± 1.21 numbers of

M6P molecules and 31.28 ± 2.01 numbers of phosphate groups coupled to each HSA molecule.

4.10.5 Conjugation of M6P-HSA to Liposomes

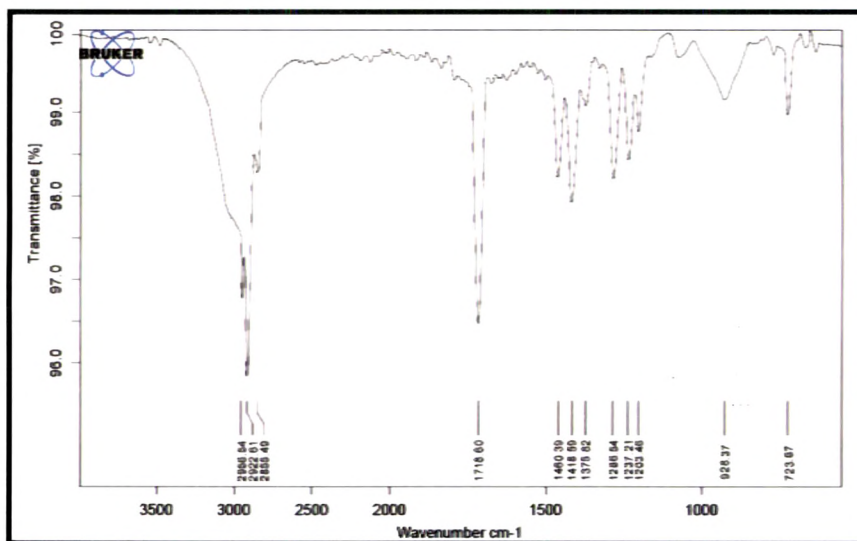


Figure 4.16 IR spectra of Sebacic acid

Presence of weak peaks at 1819.77 and 1751.16 confirms presence of (C=O) group coupled stretching. Three peaks at 1000.74, 1043.02 and 1103.61 confirms presence of (C-CO-O-CO-C) group (figure 4.17).

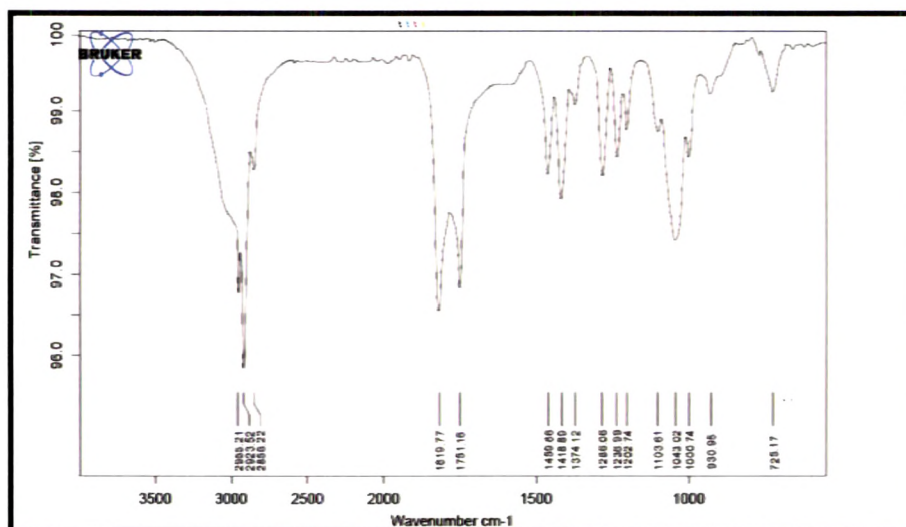


Figure 4.17 IR spectra of Sebacic anhydride

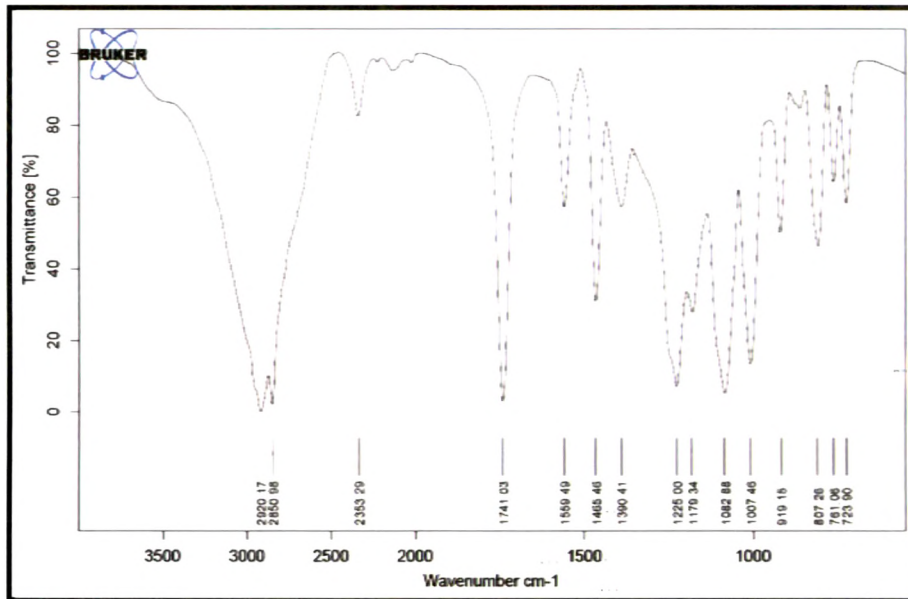


Figure 4.18 IR spectra of DSPE

Presence of a peak at 1637.48 confirms presence of (O=C-NH) group (figure 4.19).

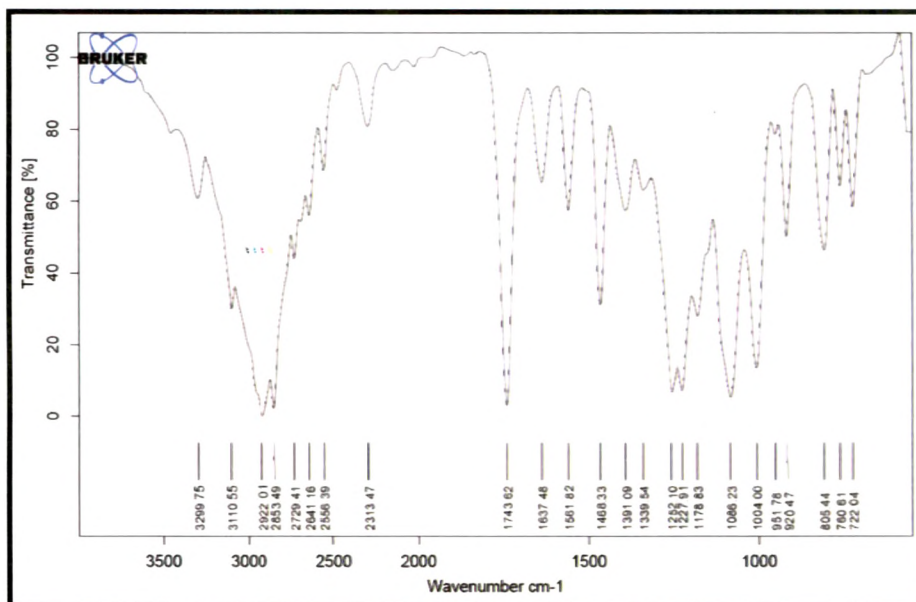


Figure 4.19 IR spectra of DSPE-Sebacic acid conjugate

4.10.6 Particle Size and Zeta Potential

The size of Liposomes was measured by dynamic light scattering with a Malvern Zetasizer. Increased particle size and zeta potential of liposomes substantiate conjugation of M6P-HSA to liposomes.

Table 4.12 Size and Zeta Potential of RGZ and CDS Liposomal Formulations

Batch	Particle size		Zeta potential (mV)
	Z-Average (d.nm)	Poly dispersity index (PDI)	
Unconjugated RGZ Liposomes	92.37 ± 3.28	0.064 ± 0.0075	-19.7 ± 1.72
M6P-HSA conjugated RGZ Liposomes	135.1 ± 3.74	0.079 ± 0.004	-30.5 ± 2.64
Unconjugated CDS Liposomes	96.45 ± 3.71	0.059 ± 0.0067	-24.4 ± 1.49
M6P-HSA conjugated CDS Liposomes	139.5 ± 3.98	0.082 ± 0.0079	-40.7 ± 1.99

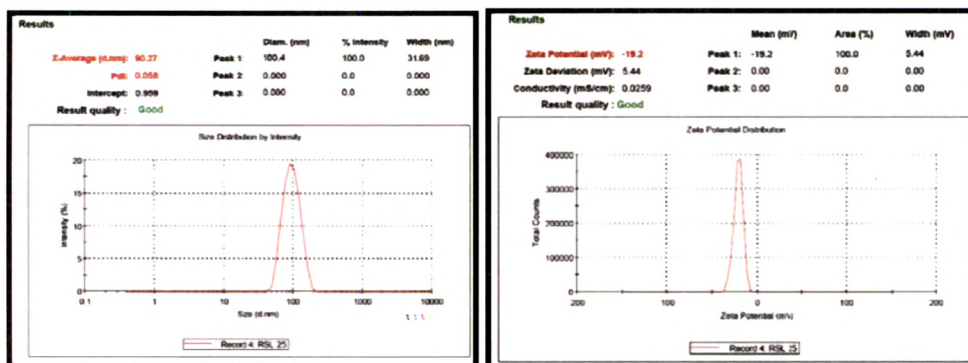


Figure 4.20 Particle size and Zeta potential of unconjugated RGZ liposomes

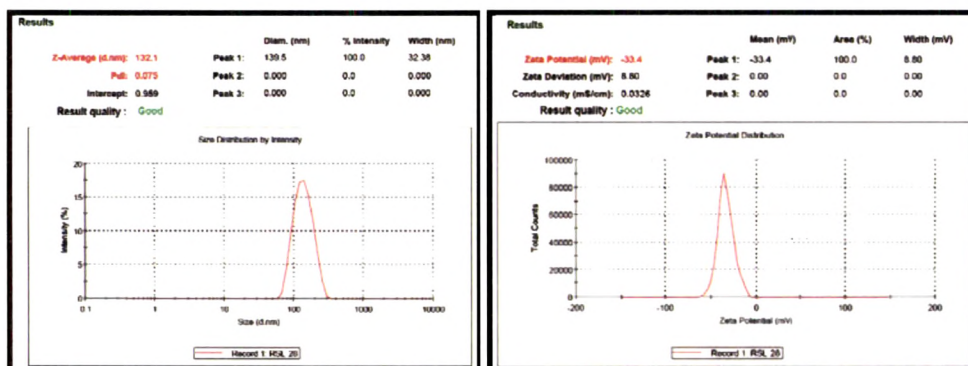


Figure 4.21 Particle size and Zeta potential of M6P-HSA conjugated RGZ liposomes

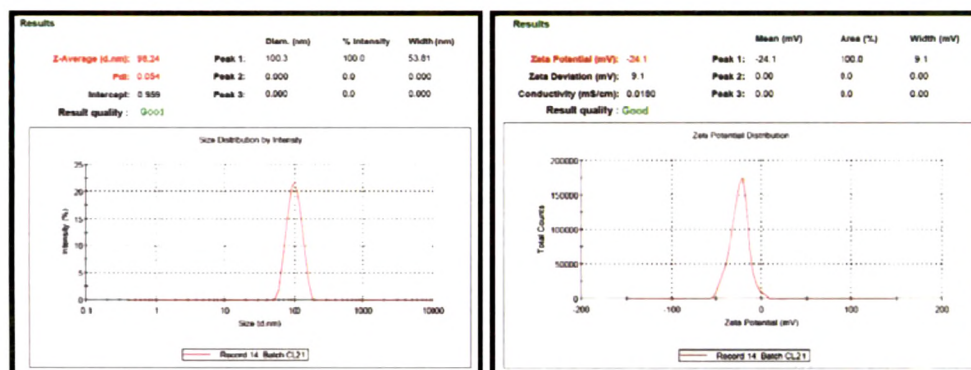


Figure 4.22 Particle size and Zeta potential of unconjugated CDS liposomes

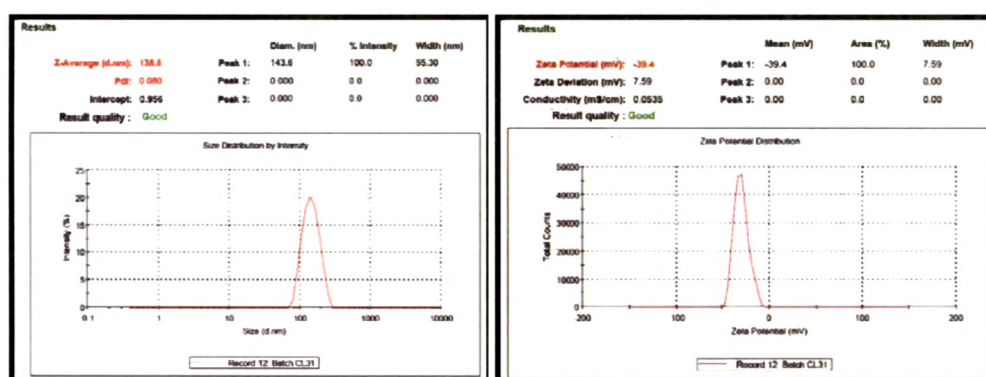


Figure 4.23 Particle size and Zeta potential of M6P-HSA conjugated CDS liposomes

4.10.7 Transmission Electron Microscopy (TEM)

The structure of liposomes was examined by TEM before and after conjugation of M6P-HSA. Liposomes had spherical shape and unilamellar structure. The liposome membranes were clearly observable because the inner aqueous compartments were slightly darker than the surrounding perimeters. The size of liposomes varied from 70 nm to 130 nm with an average diameter of 92.37 ± 3.28 nm for RGZ unconjugated liposomes (figure 4.24a) and 96.45 ± 3.71 for CDS unconjugated liposomes (figure 4.25a). The size of liposomes varied from 120 nm to 160 nm with an average diameter of 135.1 ± 3.74 nm for RGZ M6P-HSA conjugated liposomes (figure 4.24b), and 139.5 ± 3.98 for CDS M6P-HSA conjugated liposomes (figure 4.25b) measured by laser diffraction using Malvern Zetasizer. Results obtained from both TEM study and laser diffraction are parallel to each other.

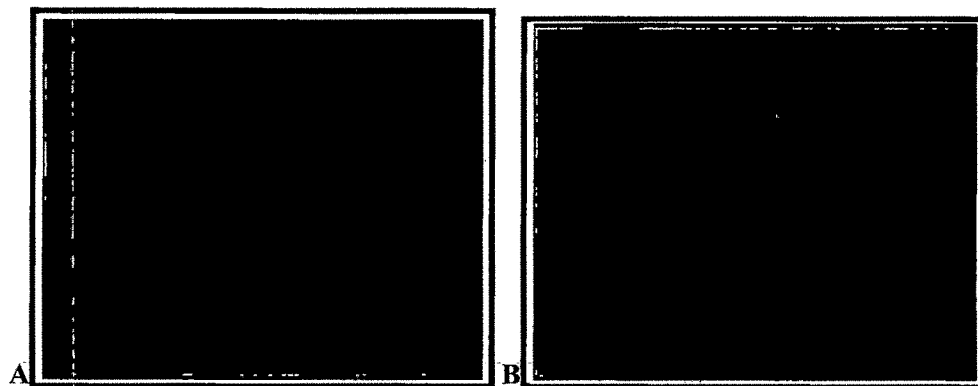


Figure 4.24 TEM images of RGZ unconjugated (A) and RGZ M6P-HSA conjugated (B) liposomes

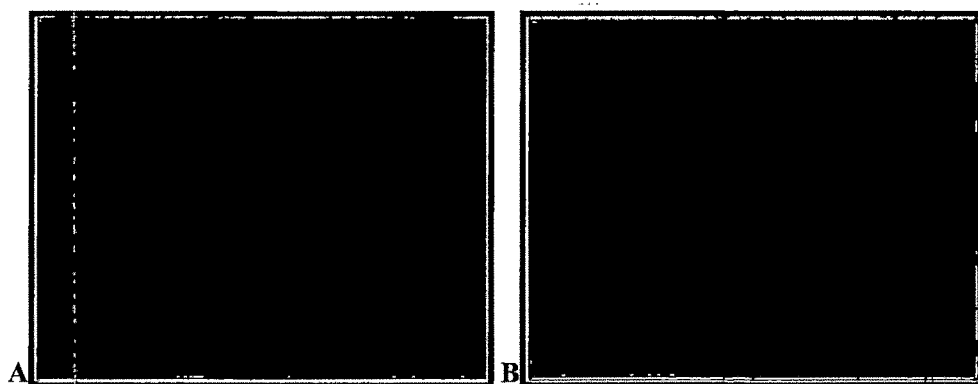


Figure 4.25 TEM images of CDS unconjugated (A) and CDS M6P-HSA conjugated (B) liposomes

4.10.8 Lyophilization of Liposomes and Optimization of Cryoprotectant Concentration

The liposomal suspensions were stabilized by lyophilization. Different cryoprotectants at various ratios and anti-adherent were evaluated. The lyophilized formulations were tested for particle size, zeta potential and percentage drug retention (PDR).

With use of sucrose as a cryoprotectant, the cake formed after lyophilization was condensed and had collapsed structure. The redispersibility of liposomes with sucrose was poor and was only possible after sonication. Particle size of liposomes was increased significantly and zeta-potential was decreased significantly after lyophilization (Table 4.13 and 4.14). The increase in the particle size could have been

due to the cohesive nature of the sucrose. Further, it was observed that the lyophilized liposomes with sucrose had tendency to absorb moisture quickly.

With mannitol and lactose, the lyophilized liposome product formed was fluffy and snow like voluminous cake. The liposomal formulation showed free flowing ability, however the redispersion was difficult and possible only after vigorous shaking. Particle size of liposomes was increased significantly and zeta-potential was decreased significantly after lyophilization (Table 4.13 and 4.14). This may be due to the low solubility of mannitol and lactose in water.

With trehalose also, the lyophilized liposomes formed fluffy and snow like voluminous cake. With trehalose as cryoprotectant, the lyophilized liposomes were redispersed easily and the increase in particle size and decrease in zeta-potential were not significant as recorded in Table 4.13 and 4.14. The redispersion of liposomes depends on the hydrophilicity of the surface. The easy redispersibility is probably due to the higher solubility of trehalose in water i.e. 0.7 parts in 1 part of water. The cryoprotective effect may be attributed to the ability of trehalose to form a glassy amorphous matrix around the liposomes, preventing the particles from sticking together during removal of water (Konan et al., 2002). Also the very property of the Tindal effect observed with liposomes was retained after redispersion of the liposomes lyophilized using trehalose. Furthermore, trehalose, a non-reducing disaccharide of glucose, has previously exhibited satisfactory cryoprotective effect for pharmaceutical and biological materials (De Jaeghere et al., 1999).

Therefore, trehalose at a ratio of 1:5 was used (as no further improvement was observed at 1:10) as a cryoprotectant and 10 % (of total solid) of glycine as antiadherent for lyophilization of optimized batches of liposomes for further studies.

Table 4.13 Lyophilization of RGZ liposomes. The data represent the mean \pm SEM (n = 3).

Different Cryoprotectants	Total solid:cryoprotectant ratio	Initial			After lyophilization								
		PDE	particle size [Z-Average (d.nm)]	Zeta potential (mV)	Percentage drug retention (PDR)	Particle size [Z-Average (d.nm)]	Zeta potential (mV)						
Lactose	1:2	71.83 \pm 0.683	135.1 \pm 3.74	-30.5 \pm 3.64	93.25 \pm 1.02	602.1 \pm 10.11	-7.7 \pm 1.10						
Sucrose					94.53 \pm 1.15	731.5 \pm 13.35	-4.6 \pm 0.92						
Mannitol					95.72 \pm 0.97	420.1 \pm 8.04	-13.2 \pm 1.23						
Trehalose					96.10 \pm 1.11	241.3 \pm 3.47	-19.2 \pm 1.78						
Lactose	1:5				71.83 \pm 0.683	135.1 \pm 3.74	-30.5 \pm 3.64	96.72 \pm 0.88	511.3 \pm 9.22	-8.3 \pm 1.01			
Sucrose								95.18 \pm 0.99	650.8 \pm 11.31	-7.0 \pm 0.98			
Mannitol								97.11 \pm 1.03	287.6 \pm 7.52	-15.8 \pm 1.21			
Trehalose								97.88 \pm 0.92	180.1 \pm 2.93	-21.9 \pm 1.33			
Lactose	1:10							71.83 \pm 0.683	135.1 \pm 3.74	-30.5 \pm 3.64	97.01 \pm 0.91	487.2 \pm 9.09	-9.0 \pm 1.13
Sucrose											95.96 \pm 1.12	632.1 \pm 10.62	-7.7 \pm 1.01
Mannitol											97.82 \pm 1.31	271.0 \pm 7.11	-16.3 \pm 1.19
Trehalose											98.12 \pm 1.22	174.3 \pm 2.62	-22.4 \pm 1.28

Table 4.14 Lyophilization of CDS liposomes. The data represent the mean \pm SEM (n = 3).

Different Cryoprotectants	Total solid:cryoprotectant ratio	Initial			After lyophilization								
		PDE	particle size [Z-Average (d.nm)]	Zeta potential (mV)	Percentage drug retention (PDR)	Particle size [Z-Average (d.nm)]	Zeta potential (mV)						
Lactose	1:2	64.01 \pm 0.772	139.5 \pm 3.98	-40.7 \pm 1.99	92.51 \pm 0.93	622.7 \pm 9.73	-10.2 \pm 0.93						
Sucrose					91.26 \pm 0.87	753.3 \pm 10.19	-6.0 \pm 0.84						
Mannitol					94.48 \pm 0.76	432.8 \pm 6.98	-17.1 \pm 1.08						
Trehalose					95.07 \pm 0.95	251.2 \pm 4.12	-25.3 \pm 1.39						
Lactose	1:5				64.01 \pm 0.772	139.5 \pm 3.98	-40.7 \pm 1.99	96.29 \pm 0.84	527.0 \pm 8.61	-11.4 \pm 0.89			
Sucrose								94.09 \pm 0.91	674.0 \pm 9.06	-9.1 \pm 0.77			
Mannitol								97.27 \pm 0.79	299.3 \pm 5.17	-21.7 \pm 1.10			
Trehalose								97.96 \pm 1.02	184.6 \pm 3.01	-29.3 \pm 1.41			
Lactose	1:10							64.01 \pm 0.772	139.5 \pm 3.98	-40.7 \pm 1.99	97.12 \pm 0.86	502.1 \pm 8.28	-12.7 \pm 0.98
Sucrose											94.74 \pm 0.72	651.7 \pm 8.89	-10.5 \pm 1.04
Mannitol											97.79 \pm 1.10	277.8 \pm 3.96	-21.9 \pm 1.09
Trehalose											98.19 \pm 0.97	180.0 \pm 2.73	-29.8 \pm 1.34

4.10.9 Solid-state Analysis

DSC curves of plain drugs and liposomal formulations are contained in figure 4.26 and 4.27. DSC curves suggest loss of drug crystallinity when drugs were loaded into the liposomes.

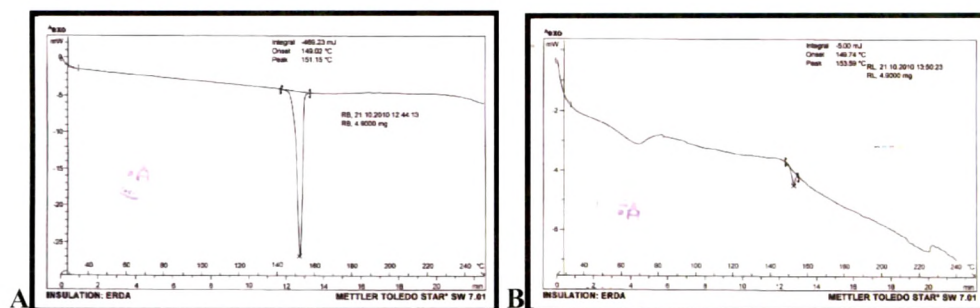


Figure 4.26 DSC curve of RGZ plain drug (A) RGZ liposomes (B)

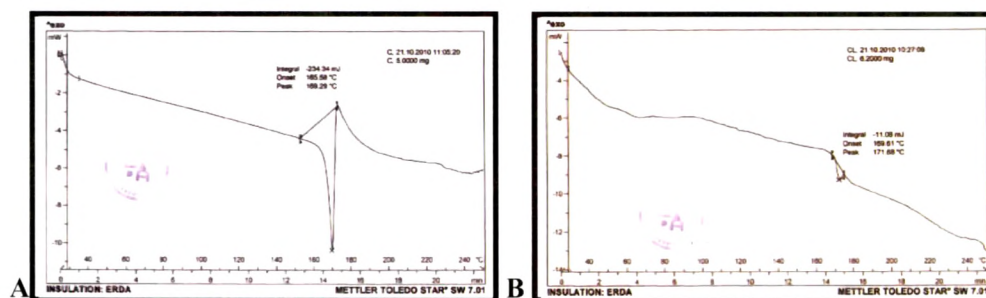


Figure 4.27 DSC curve of CDS plain drug (A) CDS liposomes (B)

X-ray diffractograms of plain drugs and liposomal formulation are demonstrated in figure 4.28 and 4.29. X-ray diffractograms showed less intensity of peaks corresponding to liposomal formulation than plain drug suggesting loss of drug crystallinity when drug was loaded into the liposomes.

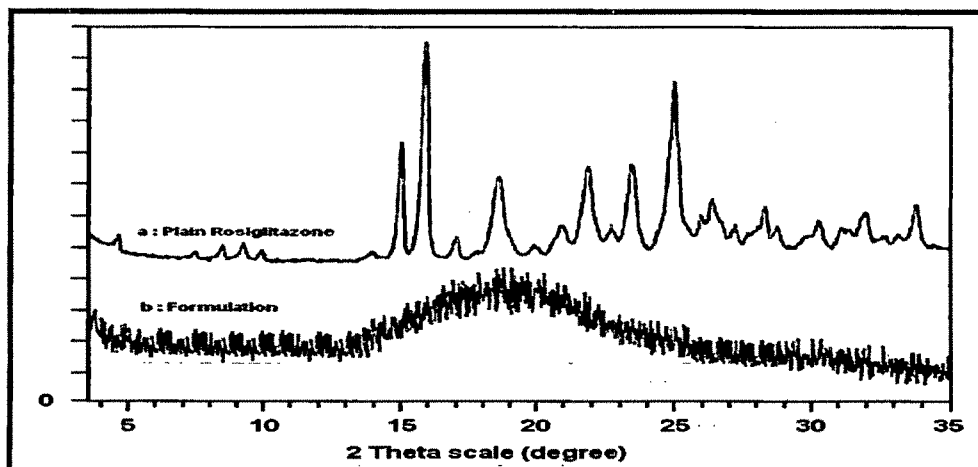


Figure 4.28 X-ray diffractograms of RGZ plain drug and liposomal formulation

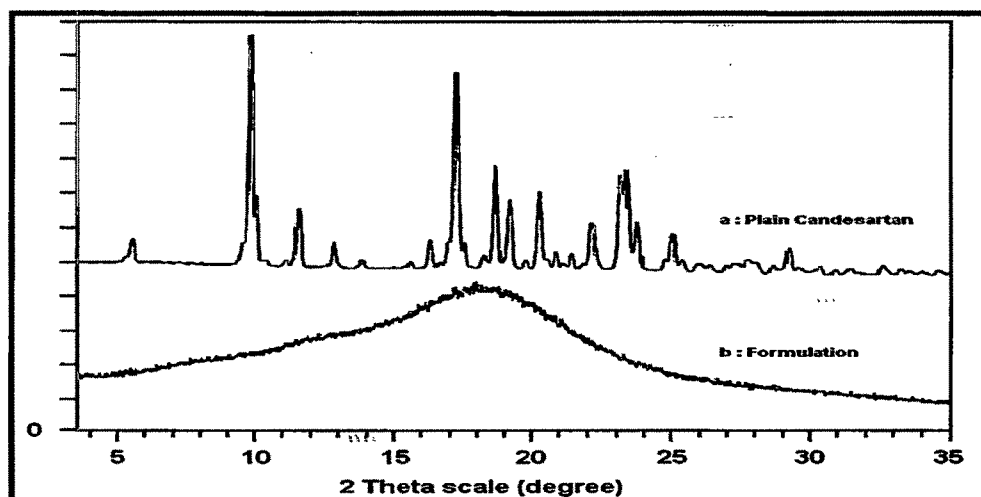


Figure 4.29 X-ray diffractograms of CDS plain drug and liposomal formulation

4.11 CONCLUSION

Liposomes of rosiglitazone and candesartan were successfully prepared by thin film hydration method. Liposomal formulations were optimized for various process and formulation variables to maximize percentage drug entrapment (PDE) and minimize percentage reduction in PDE. The liposomes were surface conjugated with M6P-HSA for potential hepatic stellate cell targeting. The optimized surface conjugated liposomal suspensions were stabilized by lyophilization.

4.12 REFERENCES

Adrian JE, Poelstra K, Scherphof GL, Molema G, Meijer DK, Reker-Smit C, Morselt HW, Kamps JA. Interaction of targeted liposomes with primary cultured hepatic stellate cells: Involvement of multiple receptor systems. *J Hepatol.* 2006 Mar;44(3):560-7.

Anthony Armstrong N, James KC. Pharmaceutical experimental design and interpretation. Taylor and Francis Publishers, Bristol, PA, USA, 1996;131-92.

Atyabi F, Farkhondehfai A, Esmaeili F, Dinarvand R. Preparation of pegylated nano-liposomal formulation containing SN-38: In vitro characterization and in vivo biodistribution in mice. *Acta Pharm.* 2009 Jun;59(2):133-44.

Bangham AD, Standish MM, Watkins JC. Diffusion of univalent ions across the lamellae of swollen phospholipids. *J Mol Biol.* 1965 Aug;13(1):238-52.

Barenholz Y, Amselem S, Lichtenberg D. A new method for preparation of phospholipid vesicles (liposomes) - French press. *FEBS Lett.* 1979 Mar 1;99(1):210-4.

Batzri S, Korn ED. Interaction of phospholipid vesicles with cells. Endocytosis and fusion as alternate mechanisms for the uptake of lipid-soluble and water-soluble molecules. *J Cell Biol.* 1975 Sep;66(3):621-34.

Beljaars L, Molema G, Weert B, Bonnema H, Olinga P, Groothuis GM, Meijer DK, Poelstra K. Albumin modified with mannose 6-phosphate: A potential carrier for selective delivery of antifibrotic drugs to rat and human hepatic stellate cells. *Hepatology.* 1999 May;29(5):1486-93.

Beljaars L, Olinga P, Molema G, de Bleser P, Geerts A, Groothuis GM, Meijer DK, Poelstra K. Characteristics of the hepatic stellate cell-selective carrier mannose 6-phosphate modified albumin (M6P(28)-HSA). *Liver.* 2001 Oct;21(5):320-8.

Betageri GV, Jenkins SA, Parsons DL. Liposome Drug Delivery Systems. PA, USA: Technomic Publishing company Inc, 1993; 16-7.

Bottecher CJF, van Gent CM, Fries C. A rapid and sensitive sub-micro phosphorous determination. *Anal Chim Acta* 1961; 24, 203-4.

- Box GEP**, Wilson KB. On the experimental attainment of optimum conditions. *J. Roy. Statist. Soc. Ser. B Metho.* 1951;13:1-45.
- Box GEP**, Hunter WG, Hunter JS. *Statistics for experiments.* John Wiley and Sons, New York, 1978;291-334.
- Cao Q**, Mak KM, Lieber CS. Dilinoleoylphosphatidylcholine prevents transforming growth factor-beta1-mediated collagen accumulation in cultured rat hepatic stellate cells. *J Lab Clin Med.* 2002 Apr;139(4):202-10.
- Cavalcanti LP**, Konovalov O, Haas H. X-ray diffraction from paclitaxel-loaded zwitterionic and cationic model membranes. *Chem Phys Lipids.* 2007 Nov;150(1):58-65.
- Cochran WG**, Cox GM. *Experimental designs.* 2nd ed; John Wiley and Sons, New York, 1992;335-75.
- Cortesi R**, Esposito E, Gambarin S, Telloli P, Menegatti E, Nastruzzi C. Preparation of liposomes by reverse-phase evaporation using alternative organic solvents. *J Microencapsul.* 1999 Mar-Apr;16(2):251-6.
- Crosasso P**, Ceruti M, Brusa P, Arpicco S, Dosio F, Cattel L. Preparation, characterization and properties of sterically stabilized paclitaxel-containing liposomes. *J Control Release.* 2000 Jan 3;63(1-2):19-30.
- Crowe LM**, Crowe JH, Rudolph A, Womersley C, Appel L. Preservation of freeze-dried liposomes by trehalose. *Arch Biochem Biophys.* 1985 Oct;242(1):240-7.
- De Bleser PJ**, Jannes P, van Buul-Offers SC, Hoogerbrugge CM, van Schravendijk CF, Niki T, Rogiers V, van den Brande JL, Wisse E, Geerts A. Insulinlike growth factor-II/mannose 6-phosphate receptor is expressed on CCl4-exposed rat fat-storing cells and facilitates activation of latent transforming growth factor-beta in cocultures with sinusoidal endothelial cells. *Hepatology.* 1995 May;21(5):1429-37.
- De Bleser PJ**, Scott CD, Niki T, Xu G, Wisse E, Geerts A. Insulin-like growth factor II/mannose 6-phosphate-receptor expression in liver and serum during acute CCl4 intoxication in the rat. *Hepatology.* 1996 Jun;23(6):1530-7.
- De Jaeghere F**, Allemann E, Leroux JC, Stevels W, Feijen J, Doelker E, Gurny R. Formulation and lyoprotection of poly(lactic acid-co-ethylene oxide) nanoparticles:

influence on physical stability and in vitro cell uptake. *Pharm Res.* 1999 Jun;16(6):859-66.

Deamer D, Bangham AD. Large volume liposomes by an ether vaporization method. *Biochim Biophys Acta.* 1976 Sep 7;443(3):629-34.

Du S, Deng Y. Studies on the encapsulation of oxymatrine into liposomes by ethanol injection and pH gradient method. *Drug Dev Ind Pharm.* 2006 Aug;32(7):791-7.

Dubois M, Gilles KA, Hamilton JK, Rebers PA, Smith F. Colorimetric method for determination of sugars and related substances. *Anal Chem.* 1956;28:350-6.

Ducat E, Brion M, Lecomte F, Evrard B, Piel G. The experimental design as practical approach to develop and optimize a formulation of peptide-loaded liposomes. *AAPS PharmSciTech.* 2010 Jun;11(2):966-75.

Fannin TE, Marcus MD, Anderson DA, Bergman HL. Use of a fractional factorial design to evaluate interactions of environmental factors affecting biodegradation rates. *Appl Environ Microbiol.* 1981 Dec;42(6):936-43.

Gonzalez-Mira E, Egea MA, Souto EB, Calpena AC, Garcia ML. Optimizing flurbiprofen-loaded NLC by central composite factorial design for ocular delivery. *Nanotechnology.* 2011 Jan 28;22(4):045101.

Gonzalez-Rodriguez ML, Barros LB, Palma J, Gonzalez-Rodriguez PL, Rabasco AM. Application of statistical experimental design to study the formulation variables influencing the coating process of lidocaine liposomes. *Int J Pharm.* 2007 Jun 7;337(1-2):336-45.

Gonzalo T, Talman EG, van de Ven A, Temming K, Greupink R, Beljaars L, Reker-Smit C, Meijer DK, Molema G, Poelstra K, Kok RJ. Selective targeting of pentoxifylline to hepatic stellate cells using a novel platinum-based linker technology. *J Control Release.* 2006 Mar 10;111(1-2):193-203.

Greupink R, Bakker HI, Bouma W, Reker-Smit C, Meijer DK, Beljaars L, Poelstra K. The antiproliferative drug doxorubicin inhibits liver fibrosis in bile duct-ligated rats and can be selectively delivered to hepatic stellate cells in vivo. *J Pharmacol Exp Ther.* 2006 May;317(2):514-21.

Greupink R, Bakker HI, Reker-Smit C, van Loenen-Weemaes AM, Kok RJ, Meijer DK, Beljaars L, Poelstra K. Studies on the targeted delivery of the antifibrogenic compound mycophenolic acid to the hepatic stellate cell. *J Hepatol.* 2005 Nov;43(5):884-92.

Hagens WI, Olinga P, Meijer DK, Groothuis GM, Beljaars L, Poelstra K. Gliotoxin non-selectively induces apoptosis in fibrotic and normal livers. *Liver Int.* 2006 Mar;26(2):232-9.

Hamilton RL Jr, Goerke J, Guo LS, Williams MC, Havel RJ. Unilamellar liposomes made with the French pressure cell: a simple preparative and semiquantitative technique. *J Lipid Res.* 1980;21(8):981-92.

Hernandez Caselles T, Villalain J, Gomez Fernandez JC. Stability of liposomes on long term storage. *J Pharm Pharmacol.* 1990;42(6):397-400.

Hinrichs WL, Mancenido FA, Sanders NN, Braeckmans K, De Smedt SC, Demeester J, Frijlink HW. The choice of a suitable oligosaccharide to prevent aggregation of PEGylated nanoparticles during freeze thawing and freeze drying. *Int J Pharm.* 2006 Mar 27;311(1-2):237-44.

Jaafar-Maalej C, Diab R, Andrieu V, Elaissari A, Fessi H. Ethanol injection method for hydrophilic and lipophilic drug-loaded liposome preparation. *J Liposome Res.* 2010;20(3):228-43.

Jiskoot W, Teerlink T, Beuvery EC, Crommelin DJ. Preparation of liposomes via detergent removal from mixed micelles by dilution. The effect of bilayer composition and process parameters on liposome characteristics. *Pharm Weekbl Sci.* 1986;8(5):259-65.

Kataoka M, Tavassoli M. Synthetic neoglycoproteins: a class of reagents for detection of sugar-recognizing substances. *J. Histochem. Cytochem.* 1984; 32(10): 1091-8.

Kenneth WY, Mark Miranda GS, Yap Wah Koon T. Formulation and optimization of two culture media for the production of tumor necrosis factor- β in *Escherichia coli*. *J Chem Technol Biotechnol.* 1995 Mar;62(3):289-94.

Kirby C, Gregoriadis G. Dehydration-Rehydration Vesicles: A Simple Method for High Yield Drug Entrapment in Liposomes. *Nat Biotechnol.* 1984;2:979-84.

Konan YN, Gurny R, Allemann E. Preparation and characterization of sterile and freeze-dried sub-200 nm nanoparticles. *Int J Pharm.* 2002;233(1-2):239-52.

Loukas YL. 2(k-p) fractional factorial design via fold over: application to optimization of novel multicomponent vesicular systems. *Analyst.* 1997;122(10):1023-7.

Maitani Y. Lipoplex formation using liposomes prepared by ethanol injection. *Methods Mol Biol.* 2010;605:393-403.

Martin FJ, Heath TD, New RRC. Chapter 4: Covalent attachment of proteins to liposomes. In: New RRC, ed. *Liposomes-A Practical Approach*. Oxford, England: IRL Press, Oxford University Press, 1990(a):163-82.

Martin FJ. Pharmaceutical manufacturing of liposomes, In: Praveen Tyle (Ed) *Specialized drug delivery systems: manufacturing and production technology*. Marcel Dekker, Inc., New York, NY, 1990(b):267-316.

Matz CE, Jonas A. Micellar complexes of human apolipoprotein A-I with phosphatidylcholines and cholesterol prepared from cholate-lipid dispersions. *J Biol Chem.* 1982 Apr 25;257(8):4535-40.

Monsigny M, Roche AC, Midoux P. Uptake of neoglycoproteins via membrane-lectin(s) of L1210 cells evidenced by quantitative flow cytometry and drug targeting. *Biol. Cell.* 1984; 51(2): 187-96.

Mu L, Feng SS. Fabrication, characterization and in vitro release of paclitaxel (Taxol) loaded poly (lactic-co-glycolic acid) microspheres prepared by spray drying technique with lipid/cholesterol emulsifiers. *J Control Release.* 2001 Oct 19;76(3):239-54.

Murthy RS, Umrethia ML. Optimization of formulation parameters for the preparation of flutamide liposomes by 3(3) factorial 26-term logit model. *Pharm Dev Technol.* 2004 Nov;9(4):369-77.

Naik S, Patel D, Surti N, Misra A. Preparation of PEGylated liposomes of docetaxel using supercritical fluid technology. *J Supercrit Fluids.* 2010;54:110-9.

New RRC. "Preparation of Liposomes" in *Liposomes: A Practical Approach*, New RRC (ed.) Oxford University Press, Oxford, 1990; 33-104.

Nounou MM, El-Khordagui L, Khallafallah N, Khalil S. Influence of different sugar cryoprotectants on the stability and physico-chemical characteristics of freeze-dried 5-fluorouracil plurilamellar vesicles. *DARU*, 2005,13(4),133-42.

Ollivon M, Lesieur S, Grabielle-Madelmont C, Paternostre M. Vesicle reconstitution from lipid-detergent mixed micelles. *Biochim Biophys Acta*. 2000 Nov 23;1508(1-2):34-50.

Ostro MJ. Liposomes. *Sci Am*. 1987 Jan;256(1):102-11.

Ozer AY, Talsma H. Preparation and stability of liposomes containing 5-fluorouracil. *Int J Pharm*. 1989 Oct 15;55(2-3):185-91.

Padamwar MN, Pokharkar VB. Development of vitamin loaded topical liposomal formulation using factorial design approach: drug deposition and stability. *Int J Pharm*. 2006 Aug 31;320(1-2):37-44.

Patel G, Chougule M, Singh M, Misra A. Chapter 9 - Nanoliposomal dry powder formulations. *Methods Enzymol*. 2009;464:167-91.

Patil MP, Gaikwad NJ. Preparation and characterization of gliclazide-polyethylene glycol 4000 solid dispersions. *Acta Pharm*. 2009 Mar;59(1):57-65.

Roche AC, Midoux P, Bouchard P, Monsigny M. Membrane lectins on human monocytes. Maturation-dependent modulation of 6-phosphomannose and mannose receptors. *FEBS Lett*. 1985 Nov 25;193(1):63-8.

Sakai H, Gotoh T, Imura T, Sakai K, Otake K, Abe M. Preparation and properties of liposomes composed of various phospholipids with different hydrophobic chains using a supercritical reverse phase evaporation method. *J Oleo Sci*. 2008;57(11):613-21.

Seltzer SE, Gregoriadis G, Dick R. Evaluation of the dehydration-rehydration method for production of contrast-carrying liposomes. *Invest Radiol*. 1988 Feb;23(2):131-8.

Seth AK, Misra A. Mathematical modelling of preparation of acyclovir liposomes: reverse phase evaporation method. *J Pharm Pharm Sci*. 2002 Sep-Dec;5(3):285-91.

Shew RL, Deamer DW. A novel method for encapsulation of macromolecules in liposomes. *Biochim Biophys Acta*. 1985 Jun 11;816(1):1-8.

Singh B, Dahiya M, Saharan V, Ahuja N. Optimizing drug delivery systems using systematic "design of experiments." Part II: retrospect and prospects. *Crit Rev Ther Drug Carrier Syst.* 2005(a);22(3):215-94.

Singh B, Kumar R, Ahuja N. Optimizing drug delivery systems using systematic "design of experiments." Part I: fundamental aspects. *Crit Rev Ther Drug Carrier Syst.* 2005(b);22(1):27-105.

Singh B, Mehta G, Kumar R, Bhatia A, Ahuja N, Katare OP. Design, development and optimization of nimesulide-loaded liposomal systems for topical application. *Curr Drug Deliv.* 2005(c) Apr;2(2):143-53.

Smirnov AA. Preparation of liposomes by reverse-phase evaporation and by freezing and thawing. *Bull Exp Biol Med.* 1984 Aug;98(2):1146-1149.

Stensrud G, Sande SA, Kristensen S, Smistad G. Formulation and characterisation of primaquine loaded liposomes prepared by a pH gradient using experimental design. *Int J Pharm.* 2000 Apr 5;198(2):213-28.

Subramanian N, Yajnik A, Murthy RS. Artificial neural network as an alternative to multiple regression analysis in optimizing formulation parameters of cytarabine liposomes. *AAPS PharmSciTech.* 2004 Feb 2;5(1):E4.

Szoka F Jr, Papahadjopoulos D. Procedure for preparation of liposomes with large internal aqueous space and high capture by reverse-phase evaporation. *Proc Natl Acad Sci U S A.* 1978 Sep;75(9):4194-8.

Vali AM, Toliyat T, Shafaghi B, Dadashzadeh S. Preparation, optimization, and characterization of topotecan loaded PEGylated liposomes using factorial design. *Drug Dev Ind Pharm.* 2008 Jan;34(1):10-23.

Van Winden EC, Talsma H, Crommelin DJ. Thermal analysis of freeze-dried liposome-carbohydrate mixtures with modulated temperature differential scanning calorimetry. *J Pharm Sci.* 1998 Feb;87(2):231-7.

Xiong Y, Guo D, Wang L, Zheng X, Zhang Y, Chen J. Development of nobiliside A loaded liposomal formulation using response surface methodology. *Int J Pharm.* 2009 Apr 17;371(1-2):197-203.

Yousefi A, Esmaeili F, Rahimian S, Atyabi F, Dinarvand R. Preparation and In Vitro Evaluation of a Pegylated Nano-Liposomal Formulation Containing Docetaxel. *Sci Pharm.* 2009 Mar 19;77:453-64.

Zasadzinski JA. Transmission electron microscopy observations of sonication-induced changes in liposome structure. *Biophys J.* 1986 Jun;49(6):1119-30.

Zumbuehl O, Weder HG. Liposomes of controllable size in the range of 40 to 180 nm by defined dialysis of lipid/detergent mixed micelles. *Biochim Biophys Acta.* 1981 Jan 8;640(1):252-62.